Reviews

Organic/Inorganic Supramolecular Assemblies and Synergy between Physical Properties†

Lahcène Ouahab

Laboratoire de Chimie du Solide et Inorganique Moléculaire UMR-CNRS 6511, Goupe Matériaux Moleculaires, Université de Rennes 1, Avenue du Général Leclerc, 35042 Rennes Cedex, France

Received February 28, 1997. Revised Manuscript Received June 5, 1997[⊗]

This paper deals with molecular materials resulting from the chemical and electrochemical molecular assemblies of organic and inorganic precursors such as organic donors derived from TTF, organic nitronyl nitroxide radicals, decamethylferrocenium, metal bis(dithiolate), metal bis(dithiolene), polyoxometalates, and hexacyanometalates. Some general aspects on molecular materials as well as constraints to design conducting and magnetic materials were recalled and supported by examples from our own contribution in the field. One of the current trends in molecular materials concerns the preparation and the study of materials combining several physical properties in a synergistic way. In this context materials with conducting and magnetic properties and also materials with spin crossover and antiferromagnetic interactions are presented.

1. Introduction

Molecular materials science is a multidisciplinary field and deals with the design and synthesis of molecule-based systems that exhibit particular physical properties such as magnetism and electrical conductivity or superconductivity.[1−6] In the recent past, these physical properties were exclusively reserved to inorganic compounds since the organic substances are in general diamagnetic and electrical insulators. However, it has been predicted theoretically and proven experimentally that some particular organic molecules exhibit magnetic properties or become electrical conductors or superconductors when they are doped or combined with other organic or inorganic moieties. In the beginning of the 1960s, Little[7] and McConnell[8] postulated respectively that it is possible to prepare molecule-based materials with superconducting and ferromagnetic T_c greater than the ambient temperature. The richness and the flexibility of molecular and coordination chemistry make these one of the current trends in this field, that deals with the design and the study of compounds exhibiting physical multiproperties, such as electrical conductivity or superconductivity and magnetism, optical and magnetic properties, spin crossover, and magnetism, in a synergistic way. Here synergy means that a given physical property could be observed only in the presence of another physical property in the same material, i.e., the two properties are correlated. The goal of this review is to report some of our contributions in this field.

The first report on the electrical conductivity in an organic solid appeared in 1954,[9,10] namely, a perylene−bromine complex, which has a room-temperature conductivity of 0.1 S cm^{-1}. In 1960, the organic acceptor TCNQ[11] was synthesized as well as a great number of its conducting charge-transfer complexes and radical ion salts.[12]

In the 1970s, the organic donor TTF[13] led to the first organic metal [TTF−TCNQ].[14,15] Its room-temperature conductivity (500 Ω^{-1} cm^{-1}) increases with the decrease of the temperature to the value of 6000 Ω^{-1} cm^{-1} at 60 K where a metal−insulator transition occurs (see Figure 1).[14,15] Since then, great interest has been devoted to this type of materials, and a great number of new organic donors and acceptors have been synthesized as well as their charge-transfer salts.

In 1979, Jerôme et al. discovered for the first time a superconducting state in $(TMTSF)_2PF_6$ at $T_c = 1.2$ K under 10 kbar.[16,17] Since then, significant improvements of T_c have been obtained in other organic salts based on either symmetrical molecules such as BEDT−TTF (or "ET")[18] or unsymmetrical ones such as DMET−TTF[19] or MDT−TTF.[20] We should mention also the acceptor-based superconductors [$M(dmit)_2$, M = Ni, Pd] series.[21] The highest T_c (12.8 K) has been observed in 1990 in κ-$(ET)_2(CuN(CN)_2)Cl$).[22] Since then, there was no improvement of this T_c in this kind of materials.

Researches on molecular conductors and ferromagnets have been conducted simultaneously. However, the first molecule based ferromagnet appeared in 1986.[23,24] Miller et al. reported the charge-transfer complex $Fe(Cp^*)_2 \cdot TCNE \cdot MeCN$[23,25,26] (Figure 2), and simultaneously Kahn et al. reported the ferrimagnetic chain $MnCu(pbaOH) \cdot H_2O)_3$.[24] We will come back to these materials in the discussion about the spin noncompensation process. The magnetic materials have progressed spectacularly since the T_c is now as high as 500 K for V_xTCNE_y[27] and 340 K for the Verdaguer's chromicya-

† Dedicated to Professor Daniel GRANDJEAN for all he has done and is still doing for the promotion of research and education in our university and elsewhere.

[⊗] Abstract published in *Advance ACS Abstracts,* August 1, 1997.

S0897-4756(97)00121-X CCC: $14.00

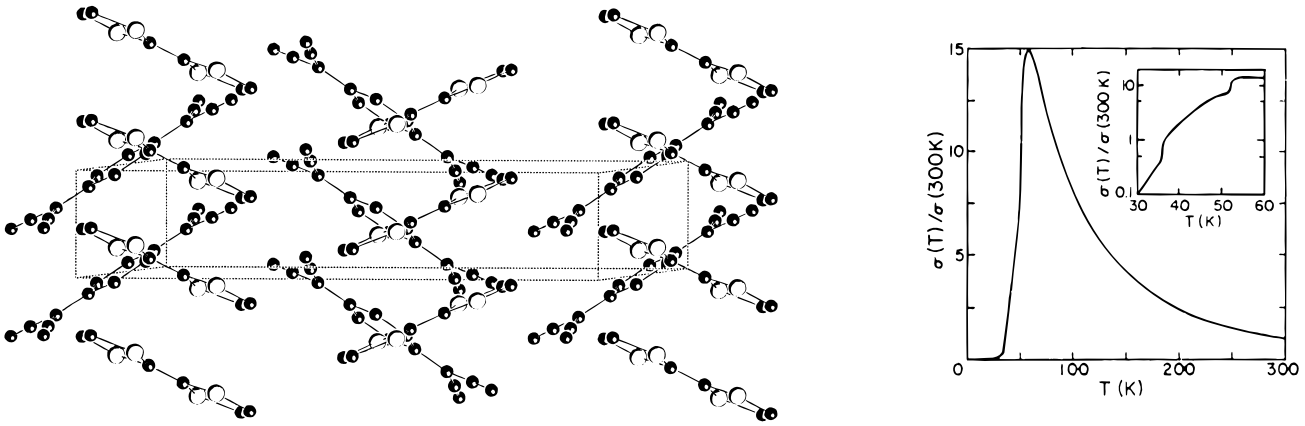

Figure 1. Crystal structure and electrical conductivity of TTF−TCNQ from refs 14 and 15.

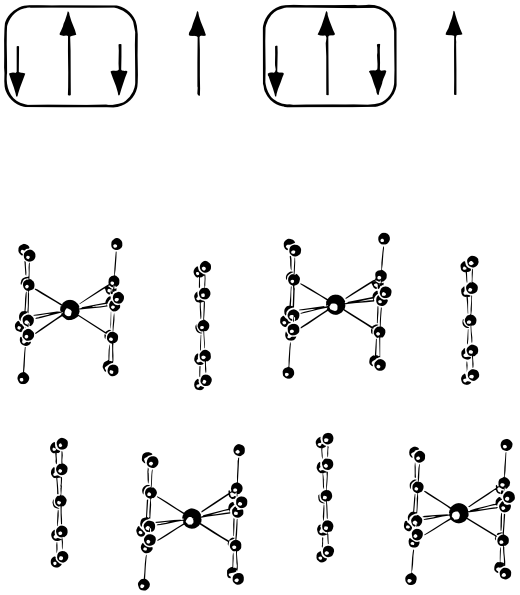

Figure 2. Crystal structure of $Fe(Cp^*)_2 \cdot TCNE \cdot CH_3CN$ and spin polarization effect according to refs 1, 23, and 25.

nure salts.[28,29]

The physical properties of a given molecular material result from the interactions between charge carriers or spin carriers. These interactions can occur through chemical bridges as in the Kahn's ferromagnets, and it can occur also through space thanks to the overlap between the π-systems of molecules such as in the organic metal TTF−TCNQ or in the Miller's ferromagnets. We are dealing in this report with magnetic and conducting materials belonging to those latter compounds with through space weak interactions. These particular classes of compounds exist as charge-transfer (CT) complexes, radical ion salts (RIS), and polymers. CT complexes are obtained by direct reaction of electron donors and electron acceptors. They are exemplified by the well-known organic metal TTF−TCNQ[14,15] and the molecule-based ferromagnet $Fe(Cp^*)_2TCNE \cdot MeCN$.[23,25,26] RIS result from the association of organic radical ions with inorganic ions, as, for example, TTF and TCNQ salts.[2,6,11−22,30]

It is well established that the dimensionality and the physical properties of a given material depend on (i) the nature of the molecular building blocks, i.e., the electronic properties such as electronic charges and redox potentials and the geometrical characteristics such as the size and the shape, and (ii) the enhancement and the interactions of these molecular blocks in the solid.

Scheme 1

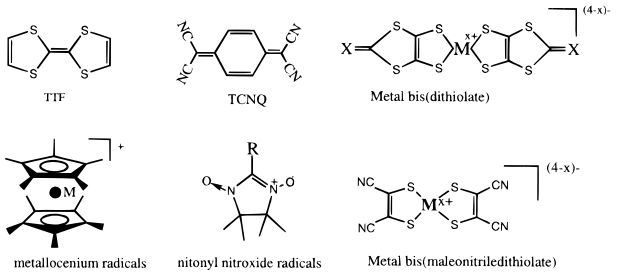

While the control of solid-state molecular organizations is more or less easy in those materials with chemical bridges between carriers, it is therefore very difficult to predict the solid-state packing for those salts with weak intermolecular bonds. For example, in TTF−TCNQ[14,15] the donor and the acceptor form separate and mixed-valence stacks giving rise to an organic metal. In $Fe(Cp^*)_2TCNE$ mixed stacks are observed, the material being insulator with a ferromagnetic transition at 4.8 K.[23,25,26] The other example concerns the BEDT−TTF salts in which several modifications are often obtained with the same synthesis conditions.[2]

2. Precursors Used

To obtain conducting and magnetic molecular materials with increased dimensionality and specific physical properties, we are investigating chemical and electrochemical molecular assemblies of particular organic and inorganic precursors (see Scheme 1). For example, TTF donor derivatives are well-known in conducting and superconducting materials.[2,6,11−22,30] Metal bis(dithiolates) are well-known in both conducting and magnetic materials.[21,31−37] Hexacyanometalates,[28,29] polyoxometalates,[38−62] metallocenium organometallic radicals,[23−26] and nitronyl nitroxide organic radicals[31,63−72] are well-known in molecular magnetism.

Before the presentation of the concerned materials, we wish to describe in more detail polyoxometalates and hexacyanometalates, which are the most used precursors in our work. To do so, we try, in the following section to answer the question: "What makes these precursors potential components in molecular materials?"

2.1. Polyoxometalates and Hexacyanometalates. *2.1.1. Common Characteristics.* Sizes and shapes: these geometrical parameters can influence the dimensionality of materials to give new molecular organizations in the solid.

Scheme 2

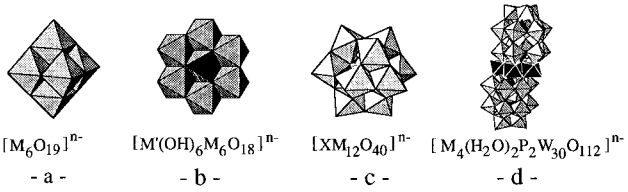

High electronic charges, which can establish strong electrostatic interactions between the molecular building blocks.

The presence of transition metals in these precursors induces a flexibility so that we can introduce paramagnetic centers, and we can also modulate their geometrical and electronic properties thanks to the coordination chemistry by changing the ligands on the metals.

These large inorganic molecular anions are soluble and stable in polar organic solvents (CH_3CN, CH_2Cl_2, ...) which make possible their electrochemical or chemical association with organic and organometallic radical cations.

2.1.2. Particular Characteristics. Polyoxometalates. Beyond the search for new materials, our goal is to obtain materials combining conducting and magnetic networks with the aim of promoting magnetic interactions via the so-called indirect exchange mechanism (described below) and also to appreciate the nature of the interactions and the influence of the delocalized electrons on the localized magnetic centers. In this contribution, we focus on the use of polyoxometalates in materials chemistry and their compositions with TTF derivatives, nitronyl nitroxide radicals, and metallocenium radicals, in the conception of conducting and/or magnetic materials.[38−57]

The polyoxometalates are easily and conveniently described as condensed MO_6 octahedra.[58−62] The most known polyoxometalates (see Scheme 2) are those that adopt the Keggin structure[73] $[(XM_{12}O_{40})^{n-}]$, the Lindqvist structure[74,75] $(M_6O_{19})^{n-}$, the Anderson−Evans structure[76,77] $[(M'(OH)_6M_6O_{18}]^{n-}$, M′ = Cr, Ni, Fe, Mn; M = Mo, W] and $[M_4(H_2O)_4(P_2W_{15}O_{56})_2)^{n-}$, M = Cu, Zn, Ni, Mn, ...] containing a M_4 transition-metal cluster encapsulated between two fragments of the trivalant Dawson−Wells structure[78−82] $(P_2W_{15}O_{56})_2$.

Polyoxometalates are inorganic electron acceptors, and it has been demonstrated that the Keggin polyoxometalate derivatives $[(XM_{12}O_{40})^{n-}]$ can accept up to 32 electrons.[83] This offers the opportunity to prepare organic donor−inorganic acceptor (ODIA) materials with a mixed valence state on the organic and inorganic units.[38−42] The reduction potentials of some polyoxometalates are given Table 1.

The potentialities of polyoxometalates are displayed in Scheme 3 through the properties of the Keggin polyoxometalates which are formulated $[(XM_{12}O_{40})^{n-}$ or $(XO_4)^{n-}M_{12}O_{36}$, M = Mo, W]. They result from the association of four M_3O_{13} units by sharing vertexes and surrounding tetrahedrally a central atom X (see Scheme 3). These polyanions present five isomers (the so-called Baker−Figgis isomers: α, β, γ, δ, and ϵ).[84] These polyanions can be diamagnetic or paramagnetic following their reduction or by substitution of the central heteroatom or one or more outer metal atoms by paramagnetic ones, and finally it is possible to substitute terminal oxygen atoms by organic ligands.[85−88]

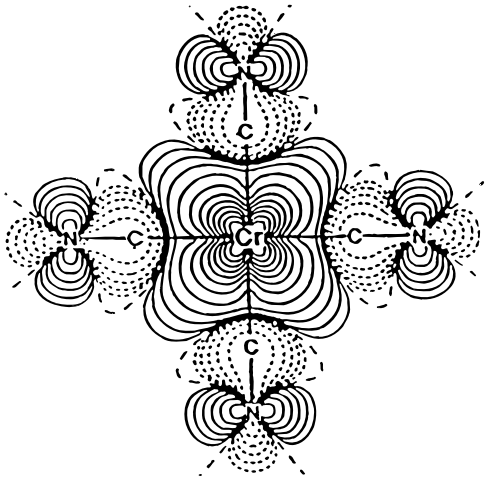

Figure 3. Spin density distribution in $Cr(CN)_6^{3-}$ from refs 89 and 90.

Scheme 3

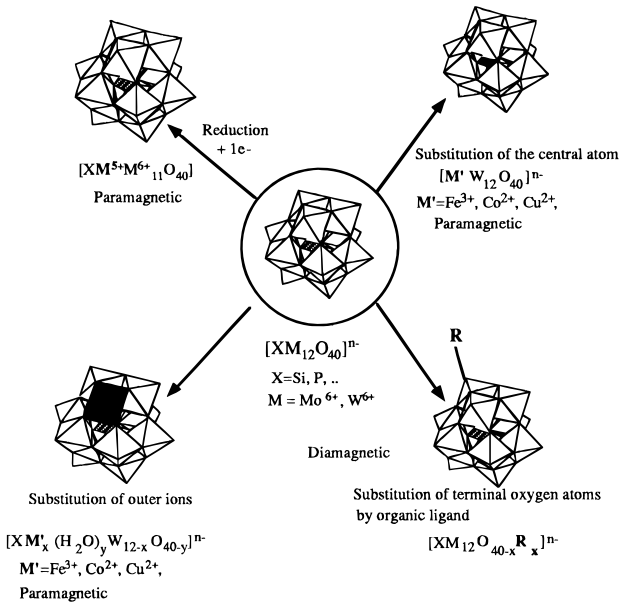

Hexacyanometalates. Thanks to $(CN)^-$ anions which are able to coordinate to transition metals, the hexacyanometalates $M(CN)_6^{3-}$ (M = Cr(III), Fe(III)) can give rise to materials with dimensionality ranging from 0 to 3D with interesting magnetic properties. In particular, Verdaguer et al. obtained molecule based ferromagnets with T_c > 300 K with this kind of precursor.[28,29]

On the other hand, the spin density distribution of the $Cr(CN)_6^{3-}$ (Figure 3) was established by Figgis et al.[89,90] from polarized neutron data, and it shows that the terminal nitrogen atom bore a significant negative spin density with an axial (or σ) symmetry with respect

Table 1. First Reduction Potential (V) of Some Polyoxometalates and TCNQ[a]

$Mo_6O_{19}^{2-}$	$W_6O_{19}^{2-}$	$PMo_{12}O_{40}^{3-}$	$PW_{12}O_{40}^{3-}$	$SiMo_{12}O_{40}^{4-}$	TCNQ	TTF
−0.3	−0.88	+0.22	−0.22	−0.25	+0.14	+0.33

[a] The first oxidation potential for TTF is also given. Values obtained by cyclic voltametry in CH_3CN, Pt electrode vs ECS, and Bu_4NBF_4 (0.1 M).

to the Cr−C−N direction.[29] Then it appears that the interaction of this negative spin with a given positive spin like that described below in the nitronyl nitroxide radicals should give rise to ferromagnetic interactions. This is what we observed in $(m\text{-rad})_3I_3(Cr(CN)_6)$[91] (see previous page).

Facile Synthesis of Tetraalkylammonium Salts. In many cases one needs to use tetraalkylammonium salts of these anions which are soluble in organic solvent. The first synthesis of $(Et_4N)_3[Fe(CN)_6]$ was reported in 1958 by Jaselski et al.,[92] by using hydrogen cyanide which is highly toxic. This synthesis was improved by Masharak[93] in 1986, according to eq 1. However this procedure

$$K_3[M(CN)_6] + 3Et_4NClO_4 \xrightarrow{CH_3OH} (Et_4N)_3[M(CN)_6] + 3KClO_4\downarrow \quad (1)$$

involves the formation of the dangerous salt $KClO_4$. This reaction is based on the precipitation of the second product of the reaction since the tetraalkylammonium salts are very soluble even in water.

Thus we have investigated another procedure conducted in two steps and based on the same principle of the precipitation of the second product of the reaction.[94] As a first step, the hexacyanometalate silver salt was synthesized in aqueous media according to eq 2. In a

$$K_3[M(CN)_6] + 3AgNO_3 \rightarrow Ag_3[M(CN)_6]\downarrow + 3KNO_3 \quad (2)$$

$$Ag_3[M(CN)_6] + 3(R_4N)I \rightarrow (R_4N)_3[M(CN)_6] + 3AgI\downarrow \quad (3)$$

second step the tetraalkylammonium salt is obtained by precipitation of the silver iodine salt ($P_s = 8.51 \times 10^{-17}$ mol L^{-1} at 25 °C in water) in water following the metathesis reaction 3.[94] The residual salt AgI was removed by filtration. The aqueous solution, which contained the soluble $(Et_4N)_3[M(CN)_6]$, was evaporated to dryness and finally the collected powder was recrystallized in acetonitrile.

3. Materials

In this section we review the design of molecular conductors and ferromagnets through theoretical mechanisms and models supported by experimental results.

3.1. Conducting Materials. The constraints to design organic conductors and the electronic and physical background of these materials are discussed in the literature.[2,30,95−97] Mainly, it is necessary to use planar open-shell molecules with delocalized π-molecular orbitals. The radical cations and radical anions of these precursors must be thermodynamically and kinetically stable with redox potential easily accessible. The best known candidates are TTF and TCNQ derivatives.

Molecular conducting materials have two unusual characteristics: (i) the organic molecules usually stack face to face to form quasi-one-dimensional and quasi-two-dimensional crystal structures, as it can be seen in Figures 1 and 4, (ii) the radical ion salts (RIS), have typical stoichiometries $(A)_m{}^-Y^{n+}$ and $(D)_m{}^+X^{n-}$, where A = organic acceptor, Y = cation, D = organic donor, X = anion, with $n/m < 1$. This stoichiometry implies a mixed-valence state on the organic systems. The role of the inorganic *monovalent* and *diamagnetic* ions (X and Y) is to offset the charge carried by the organic system. However, it has been demonstrated that the inorganic anion plays a crucial role in the dimensionality and the physical properties of materials, and consequently, some compounds with divalent, paramagnetic, and sophisticated inorganic ions appeared in the literature.[2,97−99]

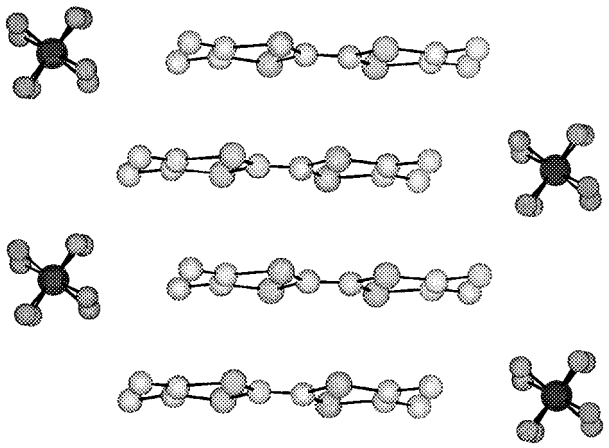

Figure 4. Crystal structure of $(TMTSF)_2X$ series from refs 16 and 17.

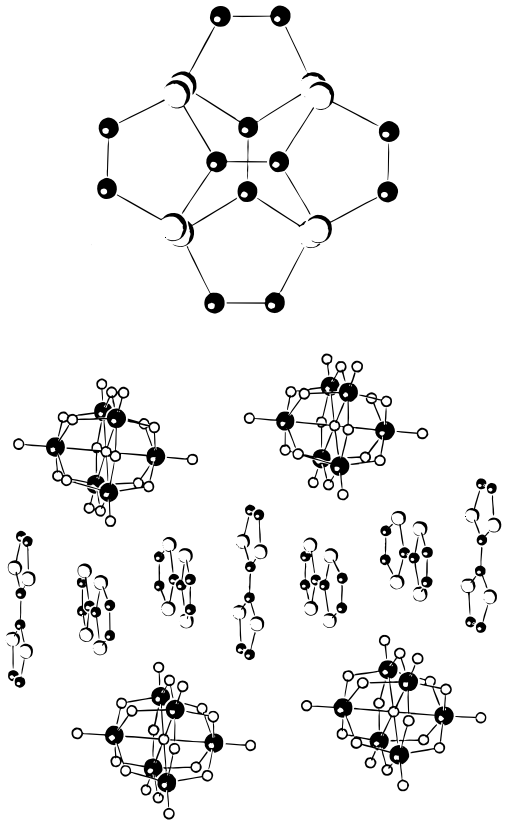

Figure 5. Crystal structure of $(TTF)_3M_6O_{19}$ and criss-cross overlap between TTFs.

TTF Derivative Salts Containing $M_6O_{19}{}^{n-}$ Lindqvist Polyoxometalates. The most important results obtained in this series concern the materials $(TTF)_3M_6O_{19}$, M = W, Mo[40,41] and $(BEDT-TTF)_5(VW_5O_{19})\cdot 8H_2O$.[53]

In the former compounds, the hybrid character of these materials is reflected in the ability of the organic chain to accommodate the size and shape of the inorganic polyanions (see Figure 5). The TTF radicals form a trimerized chain with criss-cross overlap between the adjacent molecules. These compounds are semiconductors with $\sigma_{300K} = 10^{-3}$ S cm^{-1}.

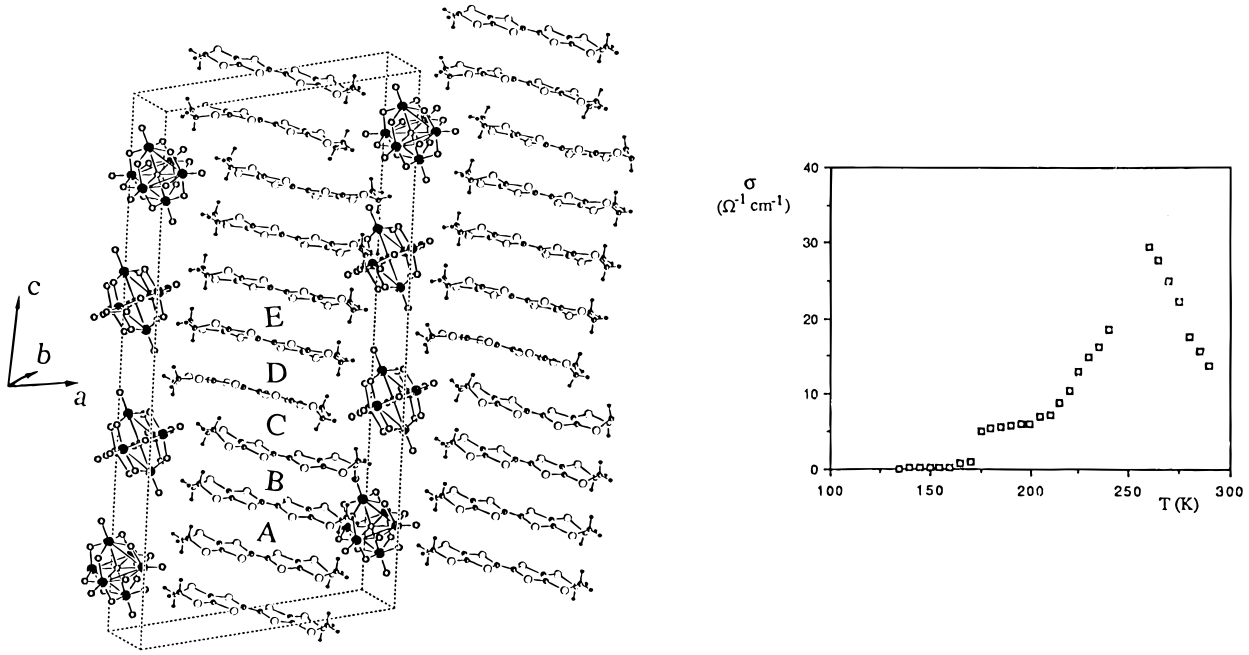

Figure 6. Crystal structure and plot of the normalized resistance versus T for $(BEDT-TTF)_5(VW_5O_{19})\cdot 8H_2O$.

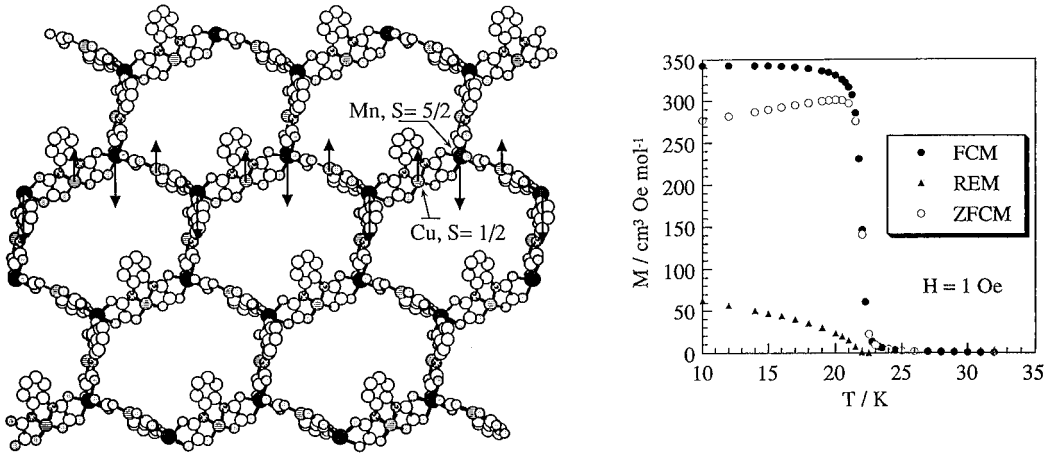

Figure 7. Structure of the anionic layers and magnetic properties of $(cat)_2Mn_2[Cu(opba)]_3$ from refs 104 and 105.

The crystal structure of the second compound (Figure 6) consists of alternate layers of organic and inorganic units. The organic layer is built from five crystallographically independent BEDT−TTF molecules noted A−E. The presence of such different organic carriers favors inhomogeneous charge distribution giving rise to charge localization and therefore poor electrical conductivities at low temperature. The plot of the normalized resistance (Figure 6) shows a metallic behavior (σ_{300K} = 12 S cm^{-1}) for this compound down to 250 K where a metal−insulator transition occurs.

3.2. Magnetic Materials. The molecule-based magnetic materials involve two kinds of compounds.[1,3−5,23−29,100−105] On one hand, we can find materials where spin−spin interactions occur through chemical bridges, the spin carriers being either transition-metal ions or both transition-metal ions and organic radicals.[1,3−5,24,28,29,100−105] On the other hand we can find materials with weak through-space interactions between isolated molecules.[1,3−5,23,25,26,63] These salts include charge-transfer complexes such as $Fe(Cp^*)_2$ −TCNE·CH_3CN[23,25,26] and radical ion salts such as those containing nitronyl−nitroxide organic radicals.[63] For this latter particular class, the magnetic interactions depend on the dimensionality of materials.

For these materials, several strategies based on spin−spin interactions are developed.[1,3−5] Some examples are cited below. A complete and detailed theoretical background on molecular magnetism is available in Kahn's book.[1] If we consider the system A−X−B where A and B are two paramagnetic centers with $S_A = S_B = 1/2$ and X a chemical bridge unabling interactions between A and B, the ground state of this system could be a singlet ($S = 0$) if the interaction is antiferromagnetic or a triplet ($S = 1$) if the interaction is ferromagnetic. The nature and the magnitude of the interaction are given by the energy difference between the singlet and triplet states $J = E_{S=0} - E_{S=1}$ ($J < 0$ for antiferromagnetic interaction and $J > 0$ for ferromagnetic interaction).

3.2.1. Spin Noncompensation Process. This mechanism consists in preparing ferrimagnetic chains or layers in which two different spin carriers alternate. This situation is encountered for instance in $(cat)_2Mn_2[Cu(opba)]_3$.[104−105] In this compound the $Mn_2[Cu(opba)]_3^{2-}$ anionic units form layers (Figure 7) in which the Cu(II) ions ($S = 1/2$) and the Mn(II) ions ($S = 5/2$) are linked by the oxamato ligands. This compound was found to be a ferromagnet with T_c = 22.5 K as shown in Figure 7. This mechanism has been used also to interpret the magnetic properties of Miller's

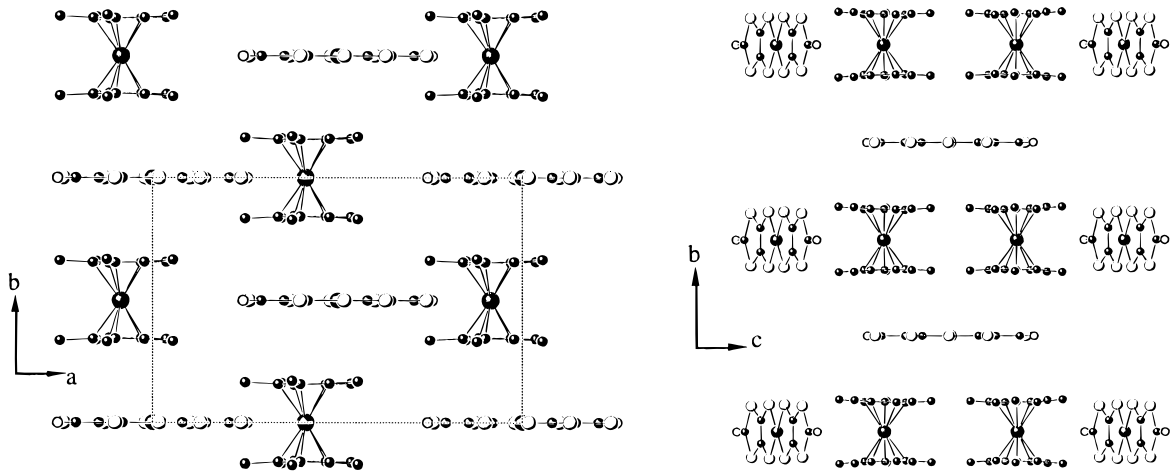

Figure 8. Crystal structure of $Fe(Cp^*)_2-Ni^{III}(dmio)_2$ from ref 112.

Scheme 4. Schematic Representation for the Stabilization of Triplet State[a]

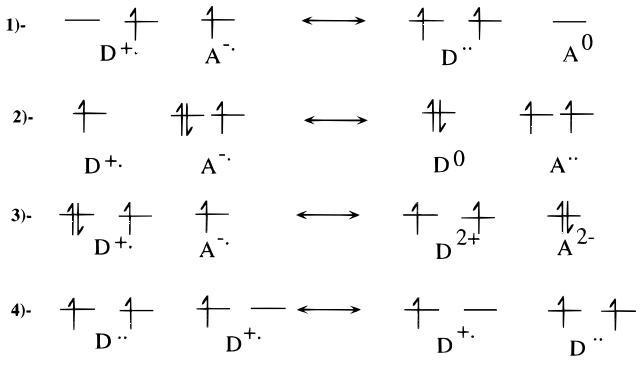

[a] (1) and (2) models from Breslow[106] and McConnell[107] concern charge-transfer salts with mixed stacks of donors and acceptors; (3) Torrance's model[108] and (4) Wudl's model[109] for radical ion salts with segregated staks of the donors and acceptors.

ferromagnet $Fe(Cp^*)_2 \cdot TCNE \cdot CH_3CN$ by considering a spin polarization effect on the $Fe(Cp^*)_2^{\bullet+}$ radical cation (Figure 2).[1,23,25,26]

3.2.2. Stabilization of the Triplet State. It has been stated by several authors[106−109] that it is possible to obtain molecule-based ferromagnets by stabilization of the triplet state in charge-transfer complexes with alternate stacks of donors and acceptors and in radical ion salts with separate stacks of the donors or acceptors and inorganic ions according to Scheme 4.[96,97,106−109]

Metallocenium organometallic radicals are fundamental building blocks of Miller's ferromagnets.[23,25−27] Besides their easily accessible reduction potentials which make them suitable molecular precursors for charge-transfer complexes, it is possible to modulate their sizes and also their magnetic moments depending on the transition metal [(from $S = {}^1/_2$ for Fe(III) to $S = {}^3/_2$ for Cr(III)]. The metallocenium salts of both polycyano organic anions and metal bis(dithiolenes) are the best examples of electron donor−acceptor (D^+A^-) charge-transfer molecular materials.[23,25−27,31−36,64,110−113]

3.2.2.1. Ferromagnetic Interactions in $Fe(Cp^*)_2$-$Ni^{III}(dmio)_2 \cdot CH_3CN$ ($dmio = S_4C_3O^{2-}$ = 2-oxo-1,3-dithiole-4,5-dithiolate). The crystal structure of this salt (Figure 8) is reminiscent of $Fe(Cp^*)_2-Ni(III)(dbs)_2 \cdot CH_3CN$, bds = $(Se_2C_6H_4)^{2-}$ = 1,2-benzenediselenolate[113] and consists of anion (A^-)−cation (D^+) mixed layers parallel to the (100) plane with the sequence ...$A^-D^+D^+A^-D^+D^+A^-$... These layers are separated in the [001] direction by anionic sheets. The structure can be regarded as an association of giant $[Ni^{III}(S_4C_3O)_2]_6$ centrosymmetrical octahedra sharing edges in the (001) plane and vertexes in the [100] direction. Each octahedron encapsulates two $Fe(Cp^*)_2^+$.[112] The magnetic properties of this salt are shown in Figure 9 as $\chi_M T$ versus T. The $\chi_M T$ product is almost constant down to 80 K and then increases more and more rapidly as the T is lowered down to 2.90 K and reaches a maximum at that temperature. When T is lowered below 2.9 K, $\chi_M T$ decreases but χ_M continues to increase and exhibits no maximum down to 1.7 K. This behavior is typical of dominant ferromagnetic interactions to which very weak antiferromagnetic interactions are superimposed. A mean field calculation leads to $J = 5.5$ cm^{-1}, J being the main value of the interaction parameter between D^+ and A^- spin carriers. The antiferromagnetic interactions are dominated by S−S intermolecular contacts. These results are in line with those reported by Broderick et al.[113] for decamethylferrocenium−Ni(III) bis(dichalcogenes). Two alternative ways have been proposed to explain these ferromagnetic interactions. Broderick et al. proposed a coupling between the D^+A^- ground state and $D^{2+}A^{2-}$ forward charge-transfer excited state, and we suggested that the interaction occurs through the overlap between the negative spin density of Cp* rings of the cations (spin polarization effect) and the positive spin density on the sulfur atoms of the anions.

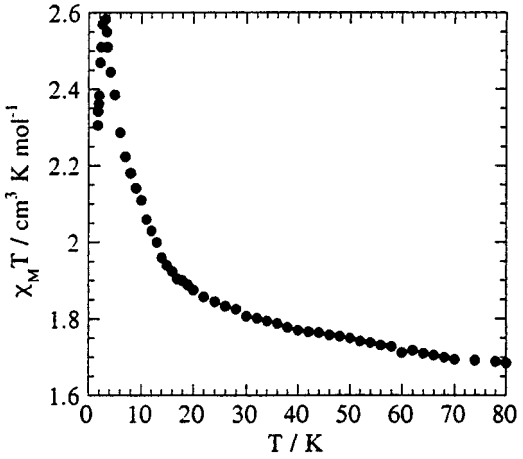

Figure 9. Magnetic properties of $Fe(Cp^*)_2-Ni^{III}(dmio)_2$ from ref 112.

3.2.2.2. Keggin Polyoxometalates and Metallocenium Radicals: $(Fe(Cp^*)_2)_4XM_{12}O_{40} \cdot n(solv)$ (X = Si, P, Fe; M

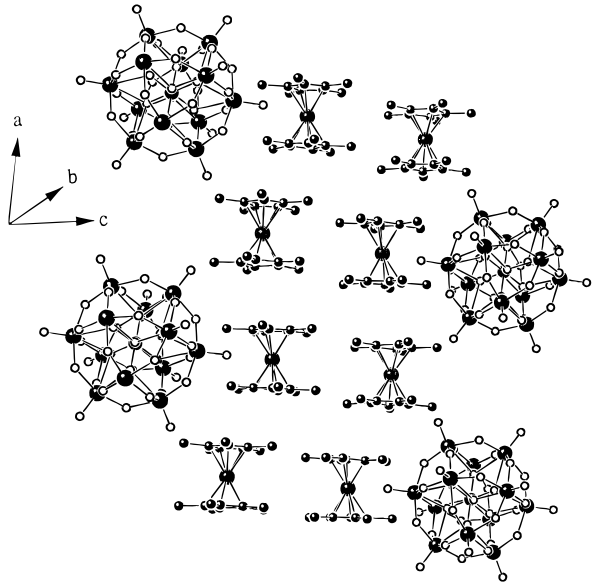

Figure 10. Evidence of 1D chains of $Fe(Cp^*)_2$ in$(Fe(Cp^*)_2)_4XM_{12}O_{40}$ from ref 56.

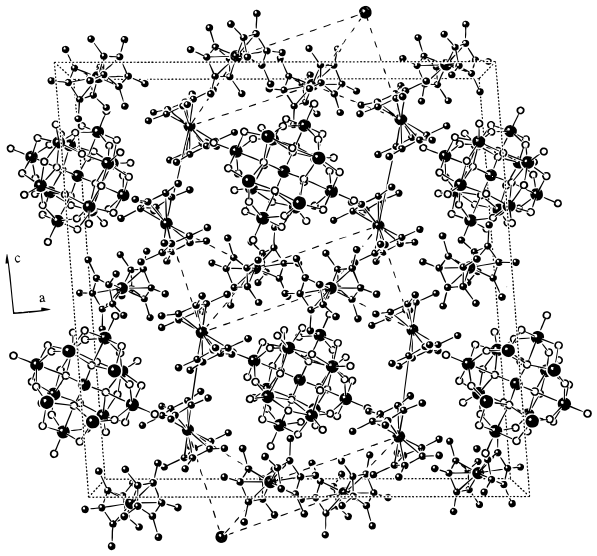

Figure 11. Evidence of $[Fe(Cp^*)_2]_{12}$ cubooctahedra encapsulating the polyoxometalate in $(Fe(Cp^*)_2)_4FeW_{12}O_{40}$ from ref 56.

= *Mo, W).* Several compounds[56] have been synthesized with both diamagnetic and paramagnetic Keggin polyanions. The general formula of these salts is $(Fe(Cp^*)_2)_4XM_{12}O_{40}\cdot n$(solv) (X = P, Si, Fe; M = W, Mo). In many cases several phases with the same stoichiometry but different crystal structures were obtained in the same batch. Two types of crystal structures were observed (Figure 10): (i) a 1D structure where $[Fe(Cp^*)_2]^+$ cations form linear chains surrounded by columns of polyoxometalates; (ii) a 3D structure where $[Fe(Cp^*)_2]^+$ occupies the vertexes of a cuboctahedron (Figure 11). The 3D structure results from the association of these cuboctahedrons by sharing vertexes in the *a* and *c* directions and sharing faces in the *b* direction. The magnetic properties of these compounds between 2 and 300 K indicate that all salts present very weak magnetic interactions obeying the Curie−Weiss expression $\chi = C/(T - \theta)$ with small values for θ (see below).[56]

3.2.2.3. Anderson−Evans Polyoxometalates and Metallocenium Radicals: $(Fe(Cp^*)_2)_3Cr(OH)_6Mo_6O_{18}\cdot 20H_2O$ Salt.[114] The Anderson−Evans type of polyoxometalate $[M'(OH)_6M_6O_{18}]^{n-}$ has two important respects: (i) this anion contains a paramagnetic ion (Cr, Ni, Fe, ...) surrounded by six MoO_6 octahedra (see Scheme 2); (ii) this polyoxoanion is planar, and therefore it can give rise to molecular solid-state organization reminiscent of $Fe(Cp^*)_2\cdot TCNE\cdot CH_3CN$[23,25,26] with an alternate stack of the $Fe(Cp^*)_2^+$ units and polyanions. The crystal structure of $(Fe(Cp^*)_2)_3Cr(OH)_6Mo_6O_{18}\cdot 20H_2O$ represented in Figure 12 is very unusual. It shows bidimensionnal layers containing orthogonal alternate stacks of the trianion and $(Fe(Cp^*)_2^+)_3$ centrosymmetric trimers with the ...(CCC)POM(CCC)POM(CCC)... sequence. In the trimer, the $(Fe(Cp^*)_2^+)$ units are perpendicular to each other. The distances between spin carriers are too large, and consequently we did not observe any magnetic interaction for this salt.

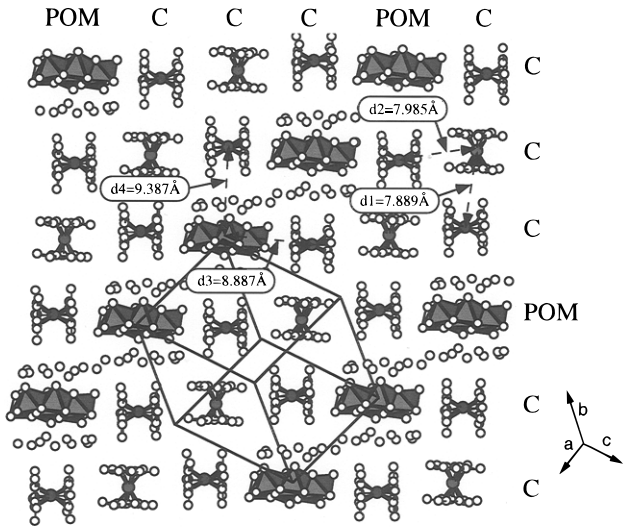

Figure 12. Crystal structure of $(Fe(Cp^*)_2)_3Cr(OH)_6Mo_6O_{18}\cdot 20H_2O$ from ref 114.

To initiate interactions in such materials, we try to decrease these separations between carriers by using smaller cations with higher magnetic moments such as $Cr(Cp)_2^{\bullet+}$ ($S = {}^3/_2$). However, while the Fe-containing metalloceniums are water and air stable, the Mn- and Cr-containing metalloceniums are very sensitive and unstable. The Anderson−Evans polyanions are stable only in water. So, as a prerequisite to this work, we synthesized very recently the salts $(Cat^+)_3Cr(OH)_6Mo_6O_{18}\cdot 6DMSO$ salts ($cat^+ = Na^+$ and Bu_4N^+)[114] that are stable in dried organic solvent.

3.2.3. Orthogonality of Orbitals. The spin interaction between unpaired electrons in orthogonal orbital is the most efficient and easiest mechanism that gives rise to ferromagnetic coupling.[1,115−117] This mechanism derives from the Hund rule, which stipulates that if two electrons occupy orthogonalized orbitals, the ground state is the high spin or the triplet state ($S = 1$). If we consider a system (A−B) with one unpaired electron on both A and B. The electron on A is described by φ_A and the electron on B by φ_B, φ_A, and φ_B being the magnetic orbitals which represent the occupied orbitals in the ground state for each molecular fragment built on A and B.[1] If φ_A and φ_B have the same symmetry (Figure 13b), the overlap integral between the two orbitals is not equal to zero. This favors the pairing of the two electrons (singlet ground state $S = 0$) to give rise to antiferromagnetic interactions. If φ_A and φ_B do not have the same symmetry (Figure 13c), they are called orthogonal. The overlap integral between the two orbitals is equal zero. In this case the Hund rule is applied, and

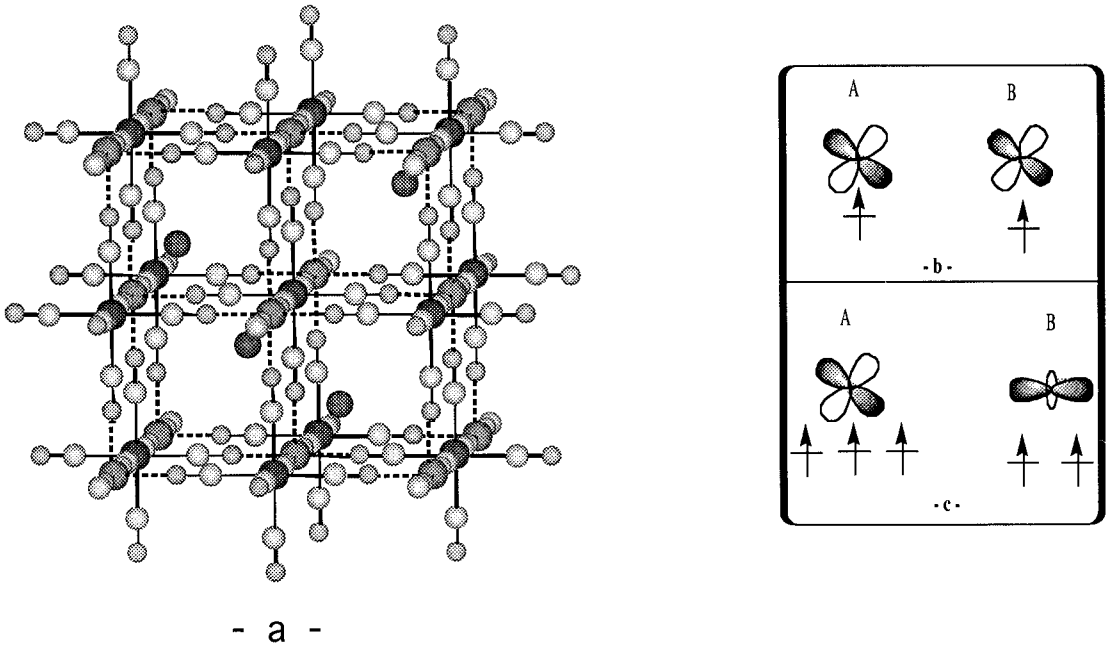

Figure 13. (a) Crystal structure of $CsNi[Cr(CN)_6]\cdot 2H_2O$, (b) orbital with same symmetry, (c) orthogonalized magnetic orbitals from refs 28 and 29. A and B represent Cr and Ni, respectively.

the ferromagnetic interactions take place. The magnitude of ferromagnetic coupling depends on the distance between orbitals.

We wish to illustrate this mechanism by several examples. The first example concerns the predictions by Verdaguer et al.[28,29] of ferromagnetic properties of Prussian blue derivatives as for example $CsNi^{II}[Cr^{III}(CN)_6]\cdot 2H_2O$ with $T_c = 90$ K.[29] The crystal structure of this compound (Figure 13a) results from the 3D connection of the $Cr(CN)_6$ units by the Ni cations. The nature of the coupling constant J was analyzed within the fragment $(CN)_5Cr-CN-Ni(NC)_5$. The Cr^{III} magnetic orbital has t_{2g} symmetry and the Ni^{II} one has e_g symmetry. They are therefore orthogonal (Figure 13c) and lead only to ferromagnetic coupling.

α-[Fe(Cp)$_2$]$_2$[M(mnt)$_2$]$_2$, M = (Fe(III), S = $^1/_2$) and (M = Co(III), S = 0).* The other example concerns the charge-transfer salts α-$[Fe(Cp^*)_2]_2[M(mnt)_2]_2$, M = (Fe(III), $S = {}^1/_2$) and (M = Co(III), $S = 0$).[64] These compounds were synthesized with the aim to obtain ferromagnetic interactions in alternate structures $(...A^-D^+A^-D^+A^-D^+...)$ of electron donors and planar electron acceptors as described in section 2. The crystal structures (Figure 14) of these α-phases show a particular and quite unusual arrangement. The $M(mnt)_2^{2-}$ units pack parallel to their main axis to build narrow columns surrounding the $Fe(Cp^*)_2^+$ ones. The $Fe(Cp^*)_2$ units are arranged in a perpendicular manner along the $(a + c)$ direction. In this configuration the overlap integral of the type $\langle e_{2g}(A)|e_{2g}(B)\rangle$ between singly occupied orbitals centered on adjacent Fe(III) centers denoted A and B are all zero, which prevent any antiferromagnetic interactions. This orthogonality of the magnetic orbitals could favor a ferromagnetic interaction which does not happen in this case for structural reasons. In fact the distances between nearest-neighbor Fe(III) centers (8.382 Å) are too long. The magnetic properties of these salts are given in Figure 15 as $\chi_M T$ versus T plot. For the salt containing diamagnetic anion (M = Co(III)), we observe a Curie Law down to low temperature. For the salts containing paramagnetic anions (M = Fe(III)), the $\chi_M T$ value

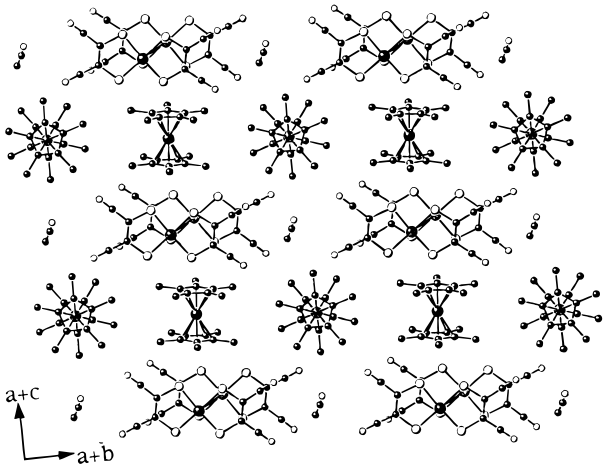

Figure 14. Crystal structure of α-$[Fe(Cp^*)_2]_2[M(mnt)_2]_2$, M = Fe(III) and Co(III).

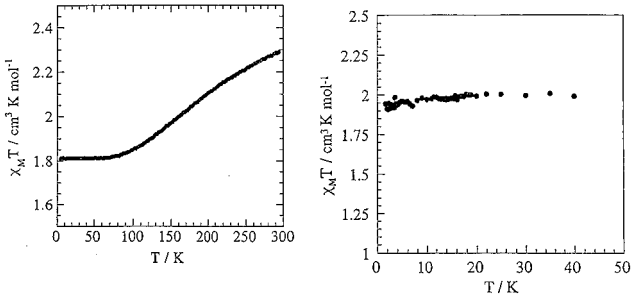

Figure 15. Magnetic properties of α-$[Fe(Cp^*)_2]_2[M(mnt)_2]_2$, M = (a) Fe(III) and (b) Co(III).

(Figure 15) decreases down to 100 K and then remains constant down to very low temperature. The first part of the plot (high temperature) is attributed to antiferromagnetic interactions between the Fe(III) ions in the anionic dimer. The second part of the plot (low temperature) is attributed to the contribution of the magnetically isolated orthogonal $Fe(Cp^*)_2^+$ units.

3.2.4. Organic Radicals and Polyradicals. Strategies based on the preparations of high-spin organic molecules are developed by several groups.[63−72] This led

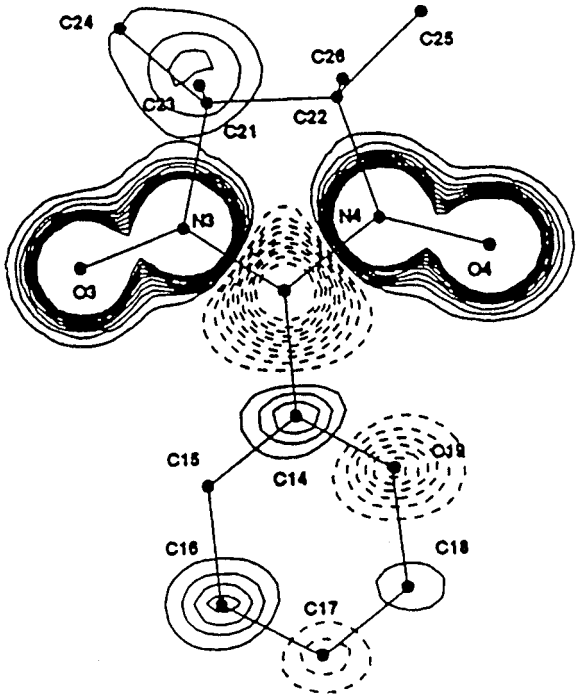

Figure 16. Spin density distribution in phenylene nitronyl nitroxide from ref 118.

to the preparation of a polycarbenic polyradical with a spin $S = 9$.[63] The first organic ferromagnet with $T_c = 0.60$ K, containing only C, H, N, O elements, is the radical *p*-nitrophenylene nitronyl nitroxide (*p*-NPNN) reported in 1991.[69,70] Organic radicals derived from nitronyl nitroxide are known to generate organic ferromagnets, and it constitutes one of the most used organic molecular building blocks in molecular magnetism.

The spin density distribution of the phenylene nitronyl nitroxide (Figure 16) was established by Schweitzer et al.[118] It shows a positive spin density on the nitrogen and oxygen atoms and a negative spin density on the sp^2 carbon atom bonded to the nitrogen atoms. This is reminiscent of the alternate spin polarization seen above in the $Fe(Cp^*)_2$ unit, and therefore this nitronyl nitroxide radical can interact with a negative spin of another carrier to give rise to ferromagnetic coupling. This is the case for example of the series $(m\text{-rad})_3I_3(M(CN)_6)$ (*m*-rad is *m*-*N*-methylpyridinium nitronyl nitroxide radical, and M = Co(III), Fe(III), Cr(III))[91] described below. Another feature of these organic radicals is their ability to undergo hydrogen bonding. This feature was used by Veciana et al. to design organic ferromagnets with various dimensionalities.[119]

3.2.4.1. Ferromagnetic Interactions in $(m\text{-rad})_3I_3(M(CN)_6)\cdot 2H_2O$ (M = Co(III), Fe(III), Cr(III)). The three compounds[91] are isostructural and crystallize in the chiral trigonal space group *P*3. In the crystal structure (Figure 17), the organic radicals (rad^+) form a sort of honeycomb lattice in the *ab* plane, consisting of three kinds of hexagons, denoted A, B, and C. The A hexagon contains one $M(CN)_6^{3-}$ anion, the B hexagon contains two iodine anions and a water molecule, and the C hexagon contains an iodine anion. This crystal structure is reminiscent of the (rad)X series reported by Awaga et al.,[120−123] where X is a combined monovalent anion such as $[(BF_4)_xI_{1-x}]^-$. There are four kinds of intermolecular interactions denoted 1−4 in Figures 17 and 18. Interactions 1−3 involve $rad^+\cdots rad^+$ units while interaction 4 involves $rad^+\cdots M(CN)_6^{3-}$ units. In interaction **1**, the two radicals are in a head-to-tail position with O···C contacts of ca. 3 Å. The same kind of interaction was observed in (rad)X series[120−123] and was found to be strongly ferromagnetic. In interaction **2** the radicals are tilted with respect to each other, with O···N and C···N contacts of ca. 3.2 Å. The same kind of interaction was also observed in (rad)X series[120−123] and was expected to give rise to antiferromagnetic coupling.[120,123,124] In interaction **3** the rad^+ units are almost perpendicular to each other with a dihedral angle between the two NOCNO mean planes of the nitronyl nitroxide groups of 92.8°. The shortest contacts occur between a nitroxide oxygen atom of a unit and both the sp^2 carbon atom and the nitroxide nitrogen atom of the other unit with O···C and O···N equal to 3.04 and 3.16 Å, respectively. This interaction may be expected to be ferromagnetic. The orthogonality of the nitronyl nitroxide groups leads to the orthogonality of the π^* singly occupied molecular orbitals (SOMO).[124,125] Furthermore, the observed O···C contact (Figure 17) may favor parallel spin alignment. Interaction **4** occurs between three symmetry related rad^+ and the cyano groups of the $M(CN)_6^{3-}$ unit with shortest N···N contacts of 3.08 Å. The C−N direction is almost perpendicular to the NOCNO mean plane of the nitronyl nitroxide groups. This interaction might favor ferromagnetic coupling since it gives rise to overlap between the positive spin density on the nitroxide groups and the negative spin density of the cyano groups (see Figure 3). The magnetic properties of these salts are shown in Figure 17 as a $\chi_M T$ versus T plot. The $\chi_M T$ values observed at room temperature correspond to what are expected for uncorrelated spins in each salt. $\chi_M T$ increases as the T is lowered to reach a maximum at

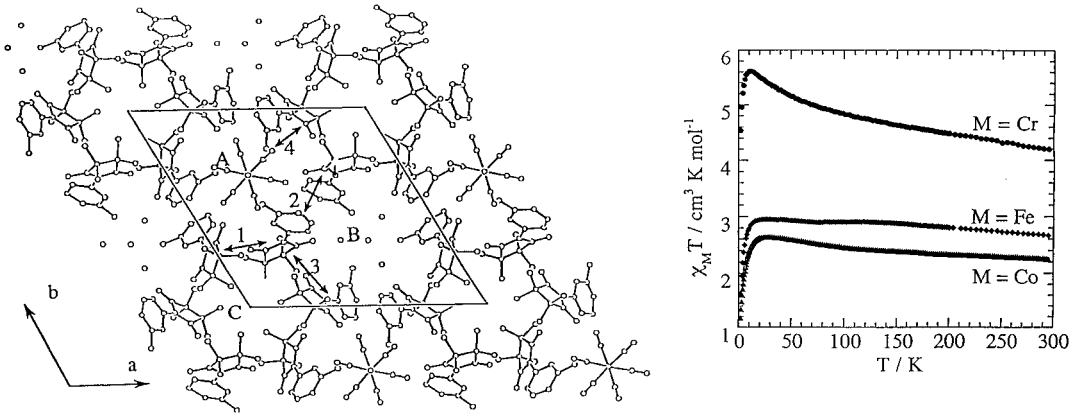

Figure 17. Crystal structure and magnetic properties of $(m\text{-rad})_3I_3(M(CN)_6)\cdot 2H_2O$ from ref 91.

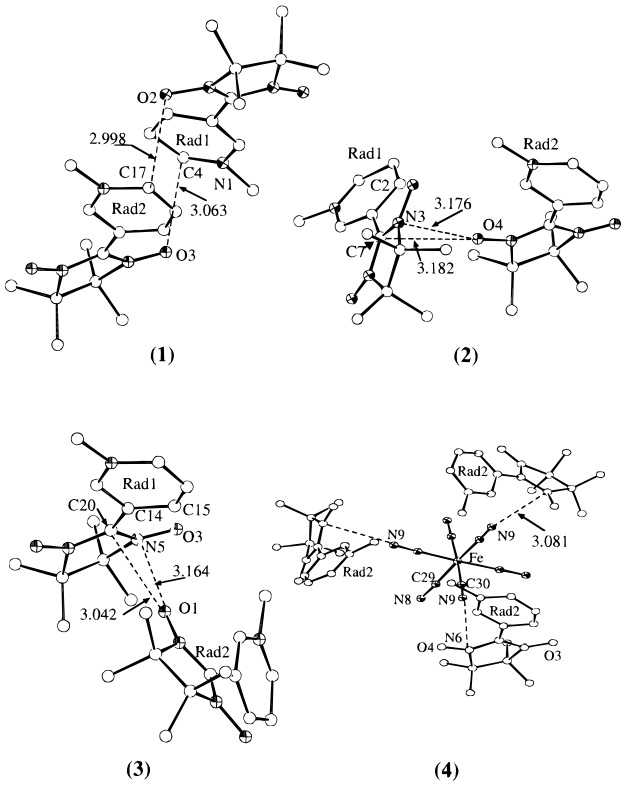

Figure 18. Details of the four kinds of interactions in $(m\text{-rad})_3I_3(M(CN)_6)\cdot 2H_2O$ from ref 91.

around 20 K and then decreases as T is lowered further. Such behaviors are characteristic of dominant ferromagnetic interactions to which antiferromagnetic interactions are superimposed.[91]

3.2.4.2. Ferromagnetic Interactions in (p-rad)$_2$[M_6O_{19}] (M = Mo, W). In the crystal structure[57] represented in Figure 19, the radicals (*p*-rad being *p*-*N*-methylpyridinium nitronyl nitroxide radical) form centrosymmetric dimers A−B which are located in the middle of the (*ab*) plane. The most significant intermolecular interactions are observed following the directions [100] and [001]. The shortest O···H distances between the radicals are 2.322(3) and 2.368(6) Å for $[Mo_6O_{19}]^{2-}$ and $[W_6O_{19}]^{2-}$, respectively. Another interesting feature in these materials concerns the interactions between the organic and inorganic units. In fact, short O···H contacts (2.20−2.30 Å) have been observed between the H atoms of the organic radical and the O atoms of the polyoxometalates, indicating the existence of hydrogen bonding in these materials (Figure 19). This result is promising as it enables us to envisage the use of paramagnetic polyoxometalates.

The magnetic properties are represented in Figure 20 in the form of the $\chi_M T$ versus T plot. The $\chi_M T$ values observed at room temperature, which correspond to what are expected for two uncorrelated radical spins, remain constant down to ca. 60 K, then increases as T is lowered further, and reaches 0.85 $cm^3\ K\ mol^{-1}$. These experimental data may be fitted with the Curie−Weiss law. Such a behavior reveals dominant ferromagnetic interactions between the radicals spins. There are three kinds of intermolecular interactions denoted 1→4 within the lattice, and it is not obvious to see which one is responsible for the observed ferromagnetic coupling. The best candidate seems to be the interaction 1 in which the nitronyl nitroxide groups are closer to each other.

4. Synergy between Physical Properties in Molecular Materials

One of the present main trends in molecular materials is to design and study compounds exhibiting multiproperties in a synergistic or complementary way. We report in this section materials combining electrical conductivity and magnetism and a new type of coordination compound with spin-crossover and magnetic interactions. But first it is important to mention the existence of many compounds showing complementarity between optical and magnetic properties and also between magnetic and photophysics.[1]

4.1. Conducting and Magnetic Materials. The aim of the combination of conductivity and magnetism in molecular materials is to obtain a long-range magnetic coupling between isolated localized spins of the inorganic networks containing transition metals (d-electrons) through the mobile electrons of the organic networks (π-electrons). This is the so-called *indirect exchange mechanism* (Scheme 5). Such magnetic coupling was observed in some transition metals and rare-earth metals and involves interactions between s-electrons and 3d- or 4f-electrons. This is the so-called RKKY (Ruderman, Kittel, Kasuya, Yoshida) model.[126,127] To match the indirect exchange model, one needs two important prerequisites, namely metallic conductors and strong interactions between the networks.

The incorporation of a localized spin in a molecular conductor has been obtained in only a few cases.[128−141] Beside the works of Miller and Epstein and co-workers cited throughout this review, it is worth noticing some of several groups' work that paved this way. Almeida et al. reported conducting materials containing paramagnetic metal bisdithiolenes,[128] and in connection with this kind of material, the important findings of Interrante et al. on the spin-Peierls of TTF−metal bisdithiolene compound.[129] The prototypical material DCNQI−Cu studied by Hunig et al.[131] and Kobayashi et al.[132] has shown of late renewed interest.[6] The other good example of conducting and magnetic material may be the Cu(pc)I (pc being phthalocyaninato) reported by Hoffman et al.[133] in which the conducting network and the paramagnetic centers are covalently linked. Let us mention also our first attempts in this field in 1984 in collaboration with Torrance on the study of TMTTF and TMTSF−$FeCl_4$ systems.[130] Finally, superconducting materials containing paramagnetic metal ions has been reported by Day et al.[137] in (BEDT−TTF)$_4$-$[(H_2O)Fe(C_2O_4)_3]C_6H_5CN$ (T_c = 8.5 K) and more recently by Kobayashi et al.[140] in $(BEDT-TTF)_2(FeCl_4)_{0.5}(GaCl_4)_{0.5}$ (T_c = 4.6 K). However, in all these compounds one of the two prerequisites mentioned above for the achievement of the indirect exchange mechanism failed, and in our knowledge, up to now there is no compound in which the synergy between conducting and magnetic properties was observed. Among the paramagnetic anions that can be used in this model, the polyoxometalates and the hexacyanometalates seem to be good candidates.

4.1.1. $[XM_{12}O_{40}]^{n-}$ Keggin Polyoxometalates. The following two series of interesting materials are worth presenting, namely, the $[(TTF)_6(Et_4N)(HXM_{12}O_{40})$, M = W, Mo; X = P, Si] and $[(BEDT-TTF)_8(M'W_{12}O_{40})$, X = Fe(III), Co(II), Cu(II), B(III), H_2^{2+}].

4.1.1.1. Evidence of Electron Transfer between the Organic Donor and the Inorganic Acceptor: [(TTF)$_6$-

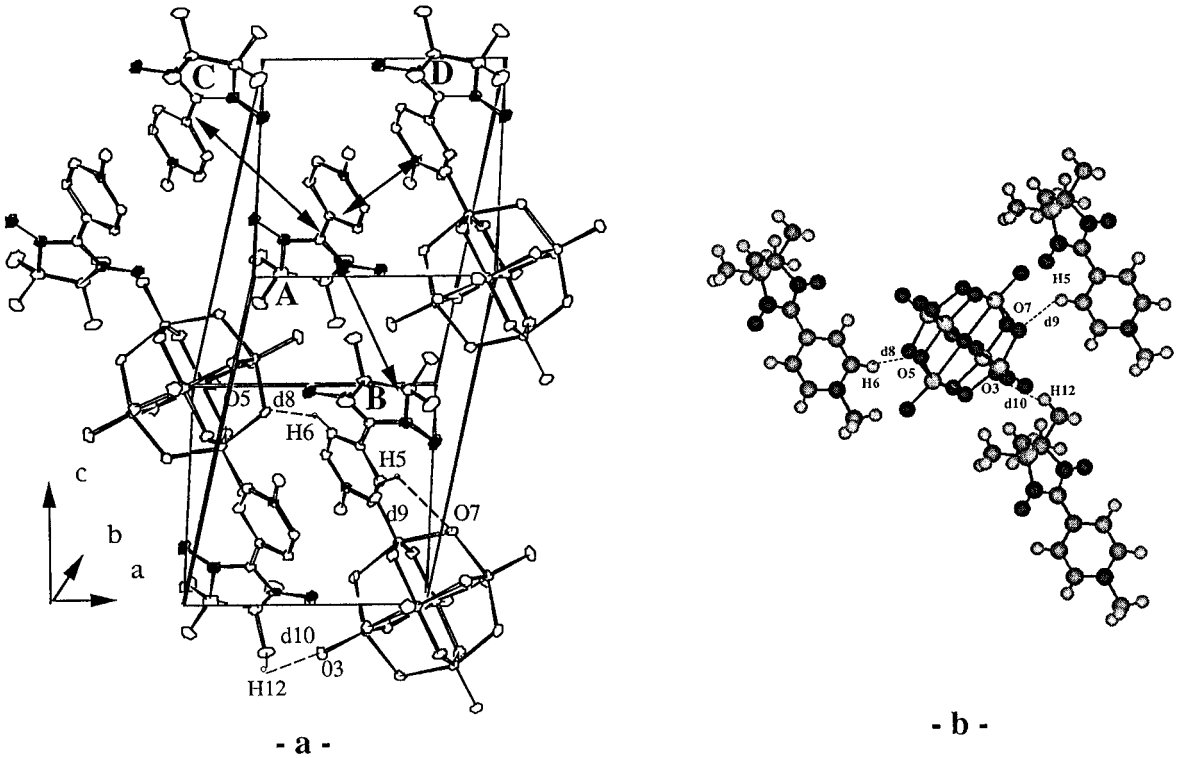

Figure 19. Projection of the crystal structure and evidence of hydrogen bonding between the organic radical and the polyoxometalate in $(p\text{-rad})_2[M_6O_{19}]$; O···H distances range from 2.20 to 2.30 Å from ref 57.

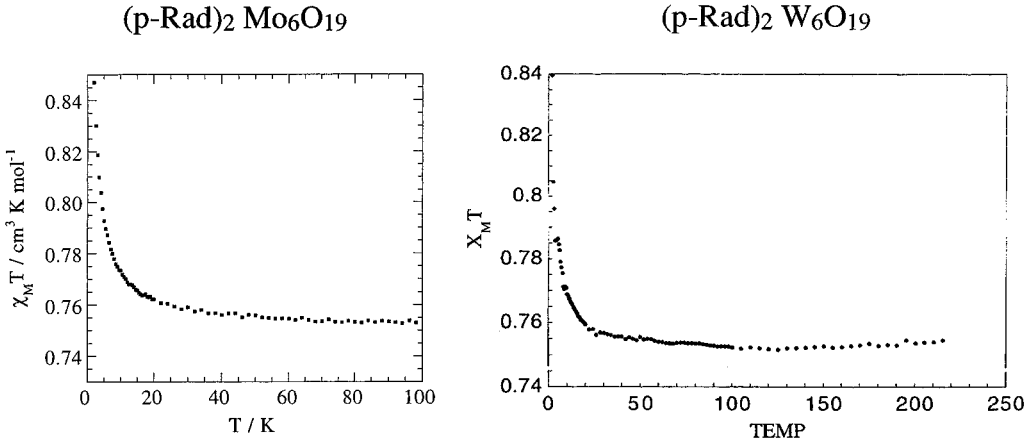

Figure 20. $\chi_M T$ versus T curve in the 2−100 K temperature range for $(p\text{-rad})_2[M_6O_{19}]$.

Scheme 5

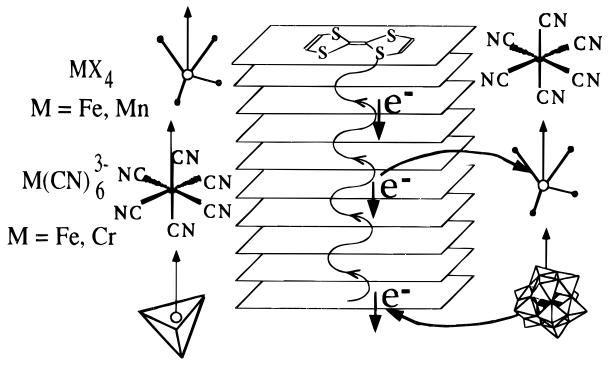

$(Et_4N)(HXM_{12}O_{40})$, M = W, Mo; X = P, Si]. In these compounds,[38,39,42] the polyoxometalates act as inorganic electron-acceptor components. In fact, the reaction of TTF with $(Et_4N)_3(PMo_{12}O_{40})$ salt gives an instantaneous dark precipitate following a redox reaction between the organic donor and the inorganic acceptor $(PMo_{12}O_{40})^{3-}$ (see eq 4). This electron transfer was evidenced in the

$$PM_{12}O_{40}^{3-} + 1e^- \rightleftharpoons PM_{12}O_{40}^{4-}$$

$$TTF^0 \rightleftharpoons TTF^{\bullet+} + 1e^- \qquad (4)$$

solid state, making the phosphometalates containing TTF salts as first materials based on paramagnetic polyoxometalates (see below).[38,39,42]

The four compounds $(TTF)_6(Et_4N)(HPMo_{12}O_{40})$ (**1**), $(TTF)_6(Et_4N)(HSiMo_{12}O_{40})$ (**2**), $(TTF)_6(Et_4N)(HPW_{12}O_{40})$ (**3**), $(TTF)_6(Et_4N)(HSiW_{12}O_{40})$ (**4**) are isostructural. The general crystal structure represented in Figure 21 is built from a polyoxoanion $XM_{12}O_{40}$ unit located at the origin of the C lattice, and three independent TTF molecules (labeled A, B, and C). The A- and B-type molecules stack regularly with an eclipsed overlap along the [001] direction, with the sequence ...ABBAAB..., in channels made of alternating polyanions and TTF molecules of the C-type (see Figure 21). The disordered $(C_2H_5)_4N^+$ cations are located on the $(00^1/_2)$ inversion center. We observed three different intrastack S···S contacts shorter than the corresponding van der Waals

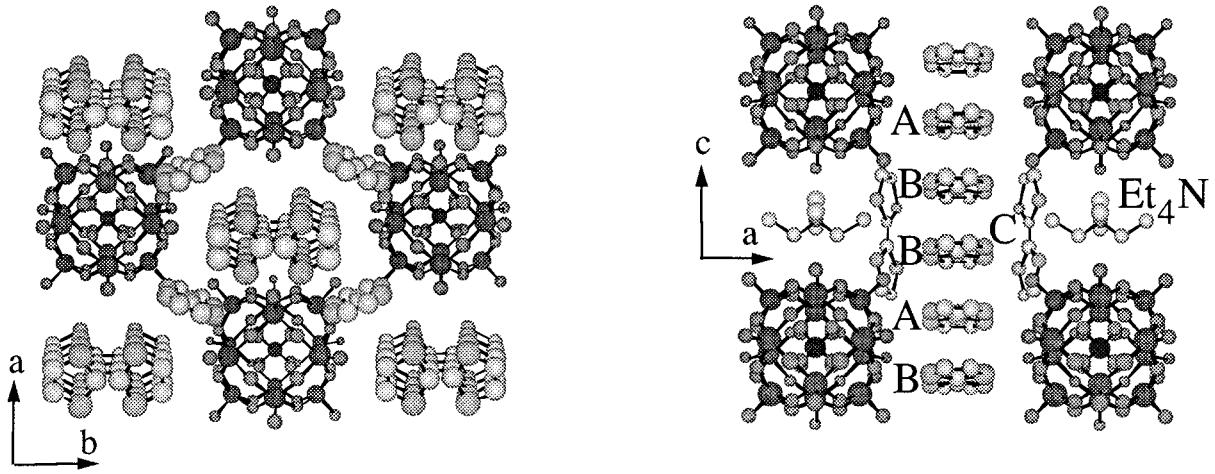

Figure 21. Projection of the crystal structure of $(TTF)_6(Et_4N)(HXM_{12}O_{40})$ materials.

separations of 3.70 Å, which suggests a slight tetramerization along the [001] direction with BAAB as a repeat unit.

All four salts present semiconducting behavior with weak room-temperature conductivities ($\sigma_{300K} = 10^{-3}$–10^{-4} S cm^{-1}). From the X-ray analysis, a simple ionic picture $(TTF)_2^0(TTF_4)^{2+}(Et_4N)^+(PM_{12}O_{40})^{3-}$ for X = P and $(TTF)_2^0(TTF_4)^{3+}(Et_4N)^+(SiM_{12}O_{40})^{4-}$ for X = Si suggests a diamagnetic behavior for the phosphorus salts and a paramagnetic behavior, due to one unpaired electron on each tetramer of the $(TTF_4)^{3+}$ sublattice, for the silicometalate ones.

However, while the silicometalate salts, **2** and **4**, exhibit a diamagnetic behavior; a temperature-dependent susceptibility was observed below 300 K for the phosphide compounds **1** and **3**. A Curie behavior was observed over a large range of temperatures. The effective moment μ_{eff} deduced from the Curie constants correspond to 1.46 and 1.49 μ_B for compounds **1** and **3**, respectively, characteristic of one unpaired electron. The reciprocal susceptibilities extrapolate to almost zero temperature showing that no magnetic interaction is occurring in these compounds.

We did not detect any intrinsic ESR signal at room temperature in any salt, which could be associated with the organic sublattice. However, when the different salts were cooled in liquid helium at 4.2 K, we observed in the case of the phosphometalate salts (**1**, **3**) an ESR signal that broadens and disappears quickly as the temperature increases. On the basis of the 4.2 K spectrum, the *g* factor equals 1.826 with a line width equal to 22 G for the compound **1**. The corresponding values are 1.947 and 15 G for **3**. These values are close to those observed in similar polyanions containing W^{5+} and Mo^{5+} ($S = {}^1/_2$) species.[142−146] On the basis of the theoretical calculations and spectroscopic, magnetic, and conducting properties, we proposed that the appropriate formula for all of the four salts is $(TTF_2)^0$-$(TTF_4)^{2+}(H)^+(Et_4N)^+(XM_{12}O_{40})^{4-}$ assuming that a proton has been trapped around the inorganic clusters during the synthesis of the salts. Consequently, we conclude that the phosphometalate anion in **1** and **3** has been reduced during the synthesis process and that the unpaired electron remains localized on a metallic site at low temperature and undergoes a rapid hopping delocalization at room temperature.

The electron transfers observed in the phosphometalate salts **1** and **3** make these salts containing mobile

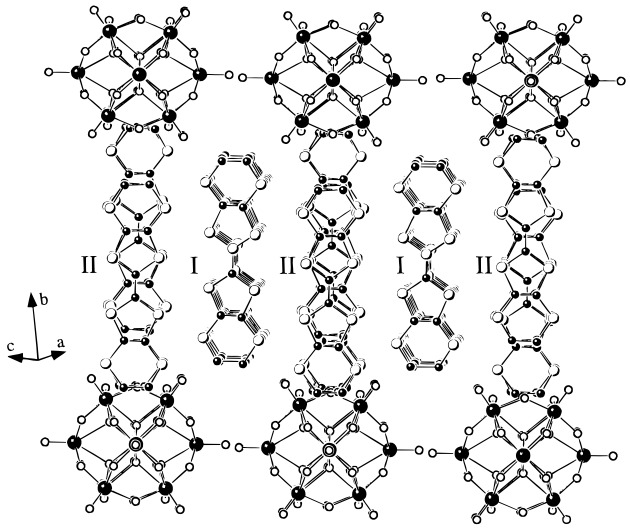

Figure 22. Crystal structures of α-$[(BEDT-TTF)_8(M'W_{12}O_{40})$ from ref 54.

electrons on the TTF stacks and localized spins on the paramagnetic polyoxometalates. These two salts match very well the indirect exchange model, but unfortunately we have not observed the expected magnetic interactions. This is probably due to the weak conductivities of the compounds.

Following these results, we decided to investigate materials with polyoxometalates containing paramagnetic transition metals (see next section).

4.1.1.2. α*-(BEDT−TTF)$_8$MW$_{12}$O$_{40}$·n(solv) (M = Fe^{3+}, Co^{2+}, Cu^2, B^{3+}, 2H$^+$, Zn^{2+}).* This work was performed with the contributions of three groups from Rennes, Bordeaux, and Valencia.[54,55]

Depending on the electrocrystallization conditions, we have obtained up to three different crystallographic phases (denoted α1, α2, and X) for nearly all the polyanions. Unfortunately all the crystals of the third phase are twinned. It is important to note the possibility of obtaining the same crystal structures in these series while we can change the anionic charge (−4 to −6) and the magnetic moment ($S = 0$ to $S = {}^5/_2$). The crystal structures of both α1 and α2 series are very similar and consist of organic and inorganic layers alternating along the [010] direction (Figure 22). The difference between the two phases concerns the packing in the *ac* plane the *b* parameter being the same for the two phases.[55] The organic network contains two dif-

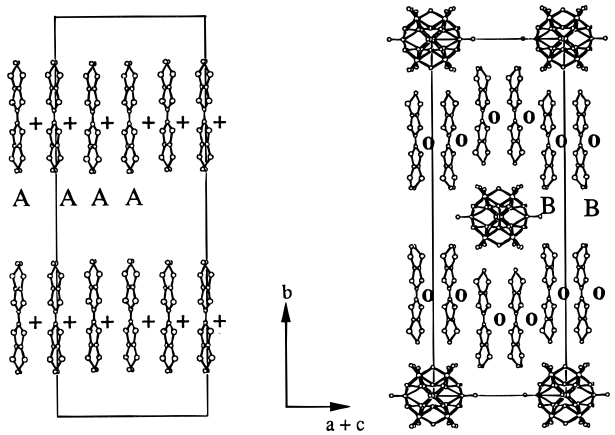

Figure 23. Evidence of the two types of organic chains in the organic layer.

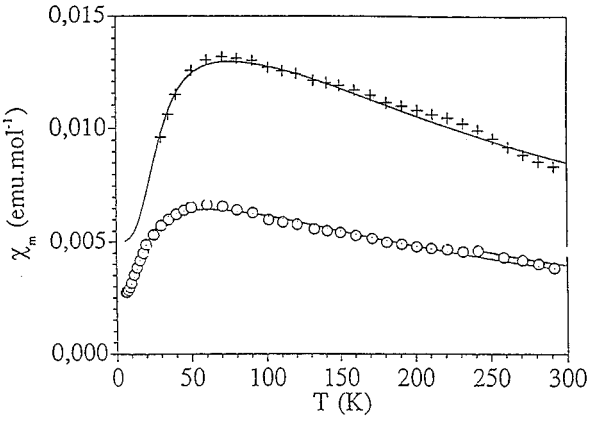

Figure 24. Plot of χ_M versus T for salts containing diamagnetic ions: α-[$(ET)_8(M'W_{12}O_{40})$]: M′ = H2 (open circles), M′ = B (crosses). Continuous lines are the best fits.

ferent BEDT−TTF chains (see Figure 22). One regular and eclipsed chain (I in Figure 23) and one dimerized chain (II in Figure 23).

From the spectroscopic properties and structural characteristics we assumed that in the eclipsed chain the BEDT−TTF molecules bear a mean charge of +1 while they are almost neutral in the dimerized chain.

The room temperature measurements made on some single crystals show dc conductivities of about 10^{-1}–10^{-3} S cm^{-1} with a semiconducting behavior in the temperature range 100−300 K. The magnetic properties of these salts have been investigated in the temperature range 4−300 K.

For those salts containing a diamagnetic ion (M′ = H_2^{2+}, Zn^{2+}, B^{3+}) a shoulder in the molar susceptibility around 60 K and a paramagnetic Curie tail at lower temperatures has been observed (Figure 24). The $\chi_M T$ versus T shows a decrease from values of 1.5−2 emu K mol^{-1} to values of 0.1−0.2 emu K mol^{-1} with the lowering of the temperature. This behavior corresponds to strong antiferromagnetic interactions between the spins of the fully oxidized BEDT−TTF chain.

In those salts containing magnetic ions (X = Cu^{II}, Co^{II}, and Fe^{III}), the $\chi_M T$ versus T (Figure 25) shows a decrease with the lowering of the temperature similar to that observed for the salts containing diamagnetic ions, reaching at low temperature the values of the corresponding isolated paramagnetic polyoxometalates deduced from their tetraethylammonium salts (see Figure 25). From these results we deduced that the same antiferromagnetic interactions occur between the

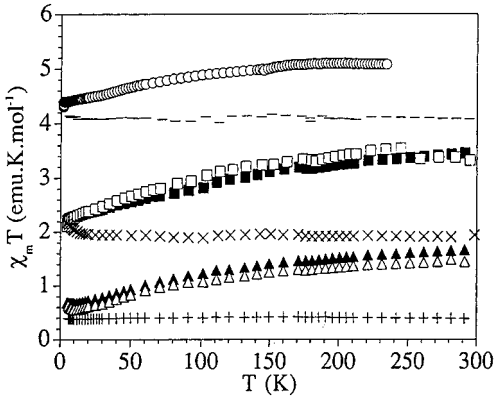

Figure 25. α1- and α2-[$(ET)_8(M'W_{12}O_{40})$]: plot of $\chi_M T$ versus T for salts containing paramagnetic ions: M′ = Cu (▲), Co (□), Fe (○). The corresponding Bu_4N^+ salts of the polyanions are also shown: M′ = Cu (+), Co (×), Fe (−).

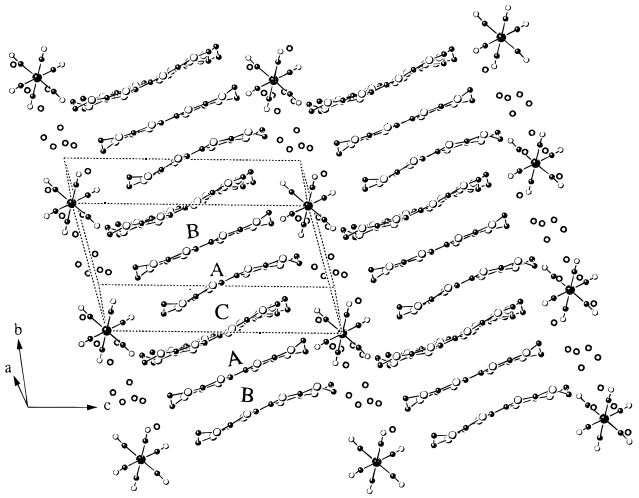

Figure 26. Crystal structure of β-$(BEDT-TTF)_5M(CN)_6$·$10H_2O$.

spins of the BEDT−TTF molecules in the fully oxidized chains and also the absence of magnetic interactions between the organic and inorganic sublattices.

4.1.2. Hexacyanometallate-Containing Materials. Molecular Assemblies of Hexacyanometalates and TTF Derivatives. The first compound reported in these systems is the insulating salt $(TTF)_{11}[Fe(CN)_6]_3$·$5H_2O$.[147] For the BEDT−TTF-based materials, depending on the experimental conditions, the electrochemical assembly with both diamagnetic hexacyanocobaltate and paramagnetic hexacyanometalates (Fe(III) and Cr(III)) yields mainly two phases formulated as β-$(BEDT-TTF)_5M(CN)_6$·$10H_2O$ and κ-$[Et_4N](BEDT-TTF)_4M(CN)_6$·$3H_2O$ (M = Fe^{III}, Co^{III}, and Cr^{III}).[94,141]

For β-phases [β-$(BEDT-TTF)_5Fe(CN)_6$·$10H_2O$], the crystal structure consists of alternating layers of BEDT−TTF and $[M(CN)_6]^{3-}$ anions (Figure 26). The inorganic sublattice is constituted by the centrosymmetric $[M(CN)_6]^{3-}$ anions, situated at the origin of the cell, and 10 water molecules. The organic sublattice is built of 2.5 crystallographically independent BEDT−TTF molecules labeled A, B, and C (Figure 26). These organic molecules form pentamerized stacks parallel to the [2,1,0] direction with the ...BACAB... sequence. These stacks form conducting sheets parallel to the (001) plane. Short S···S contacts are observed between BEDT−TTF molecules from neighboring stacks (they range from 3.325(4) to 3.617(4) Å and are shorter than

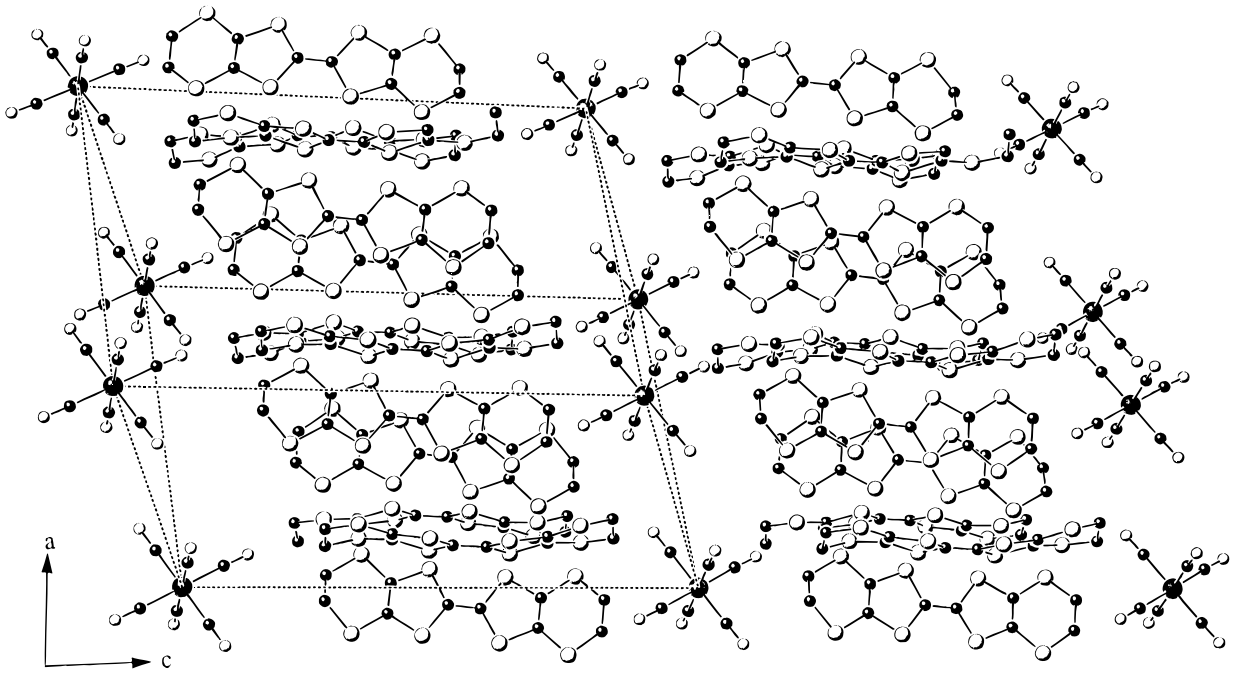

Figure 27. Crystal structure of κ-$(Et_4N)ET_4Fe(CN)_6 \cdot 3H_2O$

the sum of van der Waals radii, ≈3.65 Å). The intrastack S···S contacts are considerably longer (≥3.666(5) Å). Due to these strong side-by-side interactions, the organic molecules form "ribbons" in the [3,−1,0] direction with the same sequence ...BACAB... as that in the direction of the chains. From the comparison of the intramolecular C═C and C−S bond lengths with those of other BEDT−TTF molecules under different oxidation states, we assumed that the distribution of the charge on the BEDT−TTF molecules is irregular.

For κ-phases, the crystal structures were solved for nearly all the compounds (κ-$(Et_4N)(BEDT-TTF)_4M(CN)_6 \cdot 3H_2O$ ($M = Co^{III}$, Fe^{III}, Cr^{III})) at room temperature and ($M = Fe^{III}$, Cr^{III}) at low temperature.[94,141]

The room-temperature crystal structure shows layers of anions and organic molecules alternating in the *c* direction (see Figure 27). The centrosymmetric hexacyanometalates are situated at the origin of the cell. The trianions are connected along the *a* and *b* axis via several oxygen bridges from water molecules, creating cavities in which disordered cations $(Et_4N)^+$ are located. The organic sublattice is built of two crystallographically independent molecules, denoted A and B, which are arranged in two different kinds of dimer with a ring-to-double bond overlap in each dimer, giving rise to the first κ-phase BEDT−TTF salts involving a trianion. The intermolecular S−S contacts are very similar in both dimers. They range from 3.340(3) to 3.661(3) Å in the three salts and are shorter than the intradimer ones.

The low-temperature unit-cell parameters have been determined on single crystals for κ-$(Et_4N)(ET)_4M(CN)_6 \cdot 3H_2O$ ($M = Fe^{III}$, Co^{III}, and Cr^{III}) and studied in the range 300−115 K. In all cases, we observed a reversible doubling of the *a* parameter at about 240 K which remains unchanged down to 115 K.[94,141]

The crystal structures at low temperature were solved for the Fe^{III} and Cr^{III} salts. In both cases, the origin of the cell is displaced along the a direction so that the anions are now situated close to ($^1/_4$,0,0). Moreover, the $(Et_4N)^+$ cations show a great orientational disorder which is not solved even at low temperature. The organic sublattice is built of four crystallographically

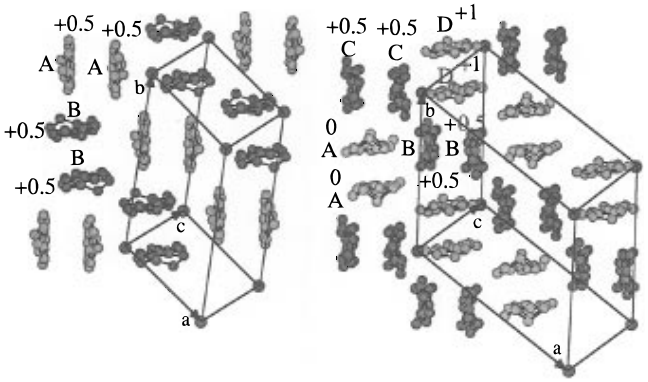

Figure 28. Charge distribution on crystallographically independent dimers in organic sublattices for κ-$(Et_4N)ET_4M(CN)_6$ at (a) room and (b) low temperature.

independent ET molecules, labeled A, B, C, and D, forming four kinds of dimers (Figure 28). The interdimer S−S distances range from 3.176(5) to 3.635(5) Å and the shortest intradimer S−S distance is 3.503(6) Å. From the intramolecular bond lengths determined by X-ray data, we can estimate that at room temperature both different ET molecules bear a charge of +0.5, whereas at low temperature one of the four different molecules is completely ionized, one other is neutral and the two last keep a charge of +0.5. Thus, the structural transition occurring at about 240 K is accompanied by a redistribution of the charges on the ET molecules, as already described in a few cases in other BEDT−TTF radical ion salts,[148−150] and is characterized by the coexistence of the organic molecules in three different oxidation states at low temperature. We assume that this charge redistribution is a dismutation in which two dimers $[BEDT-TTF^{0.5+}]_2$ built with mixed-valence BEDT−TTF radicals at room temperature change in one neutral dimer $[BEDT-TTF^0]_2$ and one other containing two completely ionized molecules $[BEDT-TTF^+]_2$ at low temperature.

The electrical conductivity measurements performed on single crystals revealed a semiconducting behavior for all salts ($\sigma_{300K} \approx 0.2-10$ S cm^{-1}).

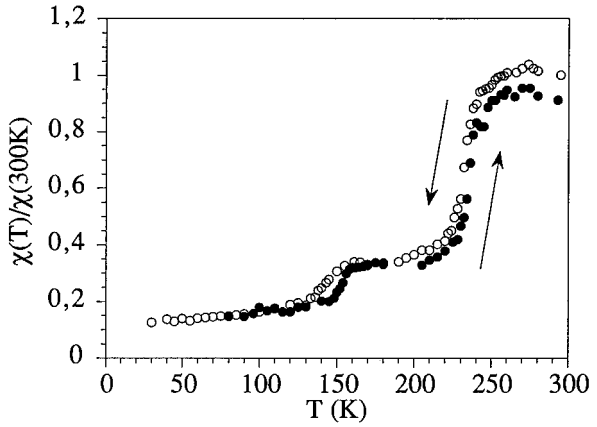

Figure 29. Normalized spin susceptibility versus T from ESR measurements for κ-$(Et_4N)ET_4Fe(CN)_6 \cdot 3H_2O$.

For the β-phases, the values of the normalized spin susceptibility calculated from the ESR spectra as well as those of the molar paramagnetic susceptibility remain unchanged in the temperature range 4.2−300 K for β phases. This behavior independent of the temperature, also called Pauli-type paramagnetism, is characteristic of conduction electrons and show the absence of significant magnetic interactions between the organic and inorganic sublattices. This is confirmed by the magnetic moment of the $Fe(CN)_6^{3-}$ containing salt which corresponds to the sum of the contributions of the paramagnetic $[Fe(CN)_6]^{3-}$ anion and the organic sublattice.

For κ-phases, the ESR spectra were carried out on single crystals for Co^{III} and Fe^{III} salts. The values of the normalized spin susceptibility and the line width calculated from the ESR spectra reveal for the Co^{III} and Fe^{III} salts two transitions at about 240 and 150 K (Figure 29). The thermal dependence of the molar paramagnetic susceptibility has been studied on the Fe^{III} compound and show the occurrence of the two transitions at about 240 and 150 K. The magnetic moment of the Fe^{III} salt corresponds to the sum of the contributions of the paramagnetic $[Fe(CN)_6]^{3-}$ anion and the organic units. This result demonstrates the absence of significant magnetic interactions between the organic and inorganic counterparts.

Difference scanning calorimetry measurements were performed between 125 and 300 K for the Fe^{III} and Co^{III} κ-salts. For both salts, the transitions are characterized by endothermic peaks. The peaks are mainly observed at about 150 K and are attributed to a first-order transition, and the calculated enthalpies are 1.5 and 0.4 J g^{-1}, respectively, for the Co^{III} and the Fe^{III} salts.

In the κ-phase salts, the decrease in the static and ESR susceptibility occurring in both transitions corresponds approximately to the loss of half of the magnetic contribution from the organic sublattice at room temperature. The first transition at about 240 K could be related to the dismutation of two ET dimers $[ET^{0.5+}]_2$ in one neutral dimer $[ET^0]_2$ and one other completely ionized $[ET^+]_2$ (see Figure 28). The neutral dimer does not have any magnetic moment, and we can assume the existence of a singlet ground state in the completely ionized ET molecules. So the magnetic contribution comes from the two other crystallographically independent ET radicals which are partially oxidized ($\rho \approx 0.5$). The second transition was not evidenced by the X-ray study; however, the DSC measurements show a very clear endothermic peak characteristic of a first-order transition, suggesting that this transition might also be accompanied by a structural modification.

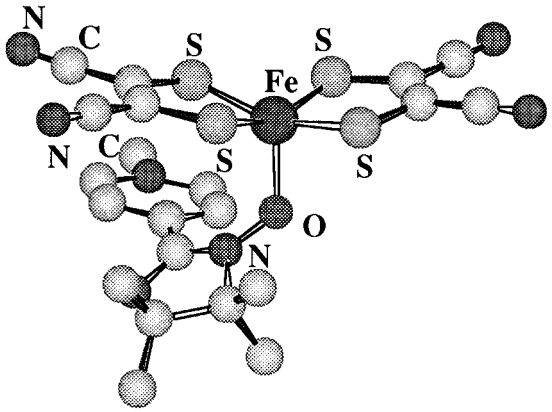

Figure 30. Molecular structure of $Fe(mnt)_2$−rad.

Scheme 6. Electronic Configuration of Fe(II) in Octahedral Ligand Field

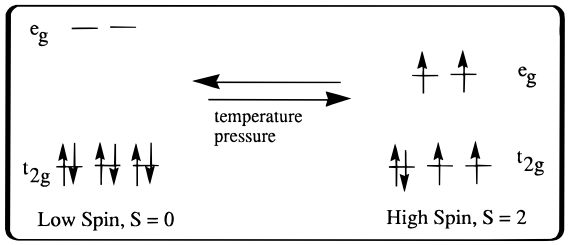

4.2. Spin Crossover and Magnetic Interactions. Two of the most important phenomena in molecular magnetism are magnetic interactions between spin carriers and spin crossover.[1,151−155] The spin crossover was discovered in 1931 by Cambi et al.[152] in iron(III) tris(dithiocarbamate). This phenomenon is observed in chemical objects that present two stable electronic states. The easy way to describe this property is to consider an iron(II) ion ($3d^6$) in an octahedral ligand field. In most cases, the energy between the T_{2g} and the e_g levels is small; the high-spin state is stabilized obeying Hund's rule; in some cases the low spin is stabilized following a temperature decrease, for example. The transition from a high-spin state to a low-spin state is followed in this case by the transfer of two electrons under the effects of temperature or pressure (see Scheme 6).

Synergy between Spin Crossover and Magnetic Interactions in Fe(mnt)$_2$−rad. The molecular structure of this compound[155] is shown in Figure 30. The rad^+ moiety [rad = 2-(*p*-*N*-methylpyridinium) 4,4,5,5-tetramethylimidazoline-1-oxyl] is linked to the iron atom of $[Fe(mnt)_2]^-$ through the oxygen atom of the nitroxide group. The Fe(III) ion adopts square-pyramidal coordination. The oxygen atom occupies the apical position. The iron atom is displaced out of the S_4 mean plane toward the apical position by 0.43 Å. All the intermolecular contacts are large, and therefore, the molecules can be considered as magnetically isolated in the crystal lattice. The temperature dependence of both χ_M (molar susceptibility) and the product $\chi_M T$ are shown in Figure 31. The value of $\chi_M T$ at room temperature corresponds to what is expected for two noninteracting spins, one ($S = {}^3/_2$) from the iron ion and the second one ($S = {}^1/_2$) for the rad^+. Below 100 K, the value of this product decreases more and more rapidly as the temperature is

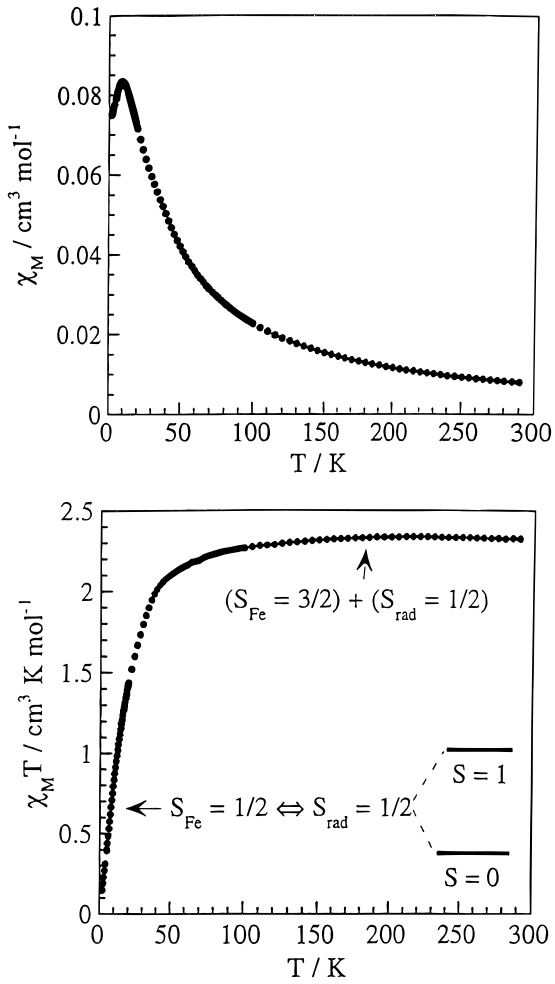

Figure 31. Temperature dependence of the molar susceptibility (χ_M) and $\chi_M T$ for Fe(mnt)$_2$−rad.

lowered. Additionally, the χ_M plot shows a pronounced maximum at $T = 9.5$, which indicates that the low-temperature ground state of this compound is a spin singlet. This nonmagnetic state can arise only from an antiferromagnetic interaction between the spin of the rad$^+$ unit ($S = {}^1/_2$) and the spin of the iron atom which should be $S = {}^1/_2$. In other word, the [Fe(mnt)$_2$]$^-$ moiety exhibits a spin crossover between $S_{Fe} = {}^3/_2$ at high temperature and $S_{Fe} = {}^1/_2$ at low temperature. It is worth noticing that this coordination compound is concerned by three features of molecular magnetism, namely, intermediate spin state, spin crossover, and antiferromagnetic interactions.

Conclusion

Molecular materials is rather a multidisciplinary field of investigations, and it involves organic, inorganic, and organometallic synthesists, solid-state chemists and physicists, theoreticians, and also researchers from industry. The fascinating flexibility of organic and coordination chemistry enables, often in very esthetic manners, molecular compatibility and assembly of organic and/or inorganic precursors that are different in many respects (size, shape, electronic charge, and intrinsic properties) and yield chemical objects with rich solid-state organizations and physical properties. The studies of these supramolecular architectures are strongly facilitated by the spectacular development of the characterization techniques.

With the few examples presented in this report, we demonstrated the potentialities of polyoxometalates, hexacyanometalates, and metal bisdithiolenes as precursors in molecular materials. The chemical and electrochemical molecular assemblies of these large polyanions with organic donors derived from TTF, nitronyl nitroxide, and metallocinium radicals led to a large variety of materials with various crystal structures and properties. We observed the following in particular:

(i) The hybrid character of the resulting compounds is reflected on one hand, through the ability of the organic sublattices to accommodate the size and the shape of the large inorganic component and on other hand in the associations of multiproperties such as electrical conductivity and magnetism or spin crossover and magnetic interactions in the same compound.

(ii) Despite the large size and high negative electronic charges of the inorganic moieties, the BEDT−TTF molecules maintain a two-dimensional packing leading to metallic behavior in (BEDT−TTF)$_5$(VW_5O_{19}), for instance.

(iii) The electron transfer from organic donors to inorganic acceptors observed in (TTF)$_6$(Et_4N)($HPM_{12}O_{40}$) giving rise to the first conducting material containing paramagnetic polyoxometalates and also to materials with mixed-valence state on the organic and inorganic counterparts.

(iv) According to the theoretical predictions, ferromagnetic couplings were observed in (*p*-rad)$_2$[M_6O_{19}] and (*m*-rad)$_3$M(CN)$_6$I$_3$ systems with through-space interactions between spin carriers.

(v) The structural richness which is reflected in the polymorphism observed in polyanion/metallocenium systems. In this respect, materials exhibiting orthogonal orbitals in Fe(Cp*)$_2$M(mnt)$_2$ or alternate layers of metallocenium radicals and planar polyoxometalates in (Fe(Cp*)$_2$)$_3$($CrMo_6O_{24}$) have been obtained, even if for crucial structural reasons, we did not observe magnetic interactions. The use of another metallocenium with lower size and higher magnetic moments will be of great interest for a systematic study of these systems.

(vi) The combination of paramagnetic inorganic polyoxometalate and hexacyanometalate anions with TTF derivatives has led to new hybrid molecular materials in which localized magnetic moments and itinerant electrons coexist. All these compounds are semiconductors and do not reveal any significant magnetic exchange between the organic and inorganic sublattices. This situation is attributed to the inhomogeneous repartition of the charges on the organic molecules. Indeed the irregular repartition of the charges induces a progressive charge localization when the temperature is lowered and accounts for the decrease in the dc conductivity values. In consequence, we assume that the weak delocalization of the conduction electrons prevents any significative interactions between the itinerant π-electrons and the localized magnetic moments of the paramagnetic inorganic polyanions. Following these results, a question still remains unravelled: "How do we improve the indirect exchange mechanism in these systems?" To give an answer to this question, we decided to investigate new materials containing organic−inorganic molecular precursors in which the organic donor and the polyoxometalate are covalently linked. This work is under current investigations in collaboration with Professor Albert Robert from our University. The results of this project will be reported elsewhere.

Acknowledgment. I am very grateful to all coworkers, whose names appear in the reference section, for fruitful collaborations and exchanges. I am indebted to all my collaborators (graduates, doctorates, postdoctorate fellows, and associate researchers) who worked hard and with enthusiasm for the realization of the results presented here: Dr. Mustapha Bencharif, Dr. Mohammed Fettouhi, Dr. Stéphane Golhen, Dr. Carlos Gomez-Garcia, Dr. Therry Le Hoerff, Dr. Pierre Le Maguerès, Dr. Allal Mhanni, Dr. Cécile Michaut, Dr. Christian Rimbaud, and Dr. Smaïl Triki.

References

(1) Kahn, O. *Molecular Magnetism*; Verlag-Chemie: New York, 1993.
(2) Williams, J. M.; Ferraro, J. R.; Thorn, R. J.; Carlson, K. D.; Geiser, U.; Wang, H. H.; Kini, A. M.; Whangbo, M.-H. *Organic Superconductors. Synthesis, Structure, Properties and Theory*; Grimes, R. N., Ed.; Prentice Hall: Englewood Cliffs, NJ, 1992.
(3) *Proceedings of the International Conference Molecule-based Magnet (ICMM'94), Mol. Cryst. Liq. Cryst.*; Miller, J. S., Epstein, A. J., Eds.; 1995.
(4) *Magnetism: a supramolecular property*; Kahn, O., Ed.; 1996.
(5) *Proceedings of the International Conference Molecule-based Magnet (ICMM'96), Mol. Cryst. Liq. Cryst.*; Itoh, Takui, Eds., in press.
(6) *Proceedings of the International Conference on Synthetic Metals (ICSM'96), Synthetic Metals*; Vardeney, Z. V., Epstein, A. J., Eds., in press.
(7) Little, W. A. *Phys. Rev*. **1964**, *134A*, 1416.
(8) McConnell, H. M. *J. Chem. Phys.* **1963**, *39*, 1910.
(9) Akamatu, H.; Inokuchi, H.; Matsunaga, Y. *Nature (London)* **1954**, *173*, 168.
(10) Akamatu, H.; Inokuchi, H.; Matsunaga, Y. *Bull. Chem. Soc. Jpn.* **1956**, *29*, 213.
(11) Acker, D. S.; Harder, R. J.; Hertler, W. R.; Mahler, W.; Melby, L. R.; Benson, R. E.; Mochel, W. E. *J. Am. Chem. Soc.* **1960**, *82*, 6408.
(12) Melby, L. R.; Harder, R. J.; Hertler, W. R.; Mahler, W.; Benson, R. E.; Mochel, W. E. *J. Am. Chem. Soc.* **1962**, *84*, 3374.
(13) Wudl, F.; Smith, G. M.; Hufnagel, E. J. *J. Chem. Soc., Chem. Commun.* **1970**, 1453.
(14) Ferraris, J.; Cowan, D. O.; Walatka, V.; Perlstein, J. H. *J. Am. Chem. Soc.* **1973**, *95*, 498.
(15) Coleman, L. B.; Cohen, M. J.; Sandman, D. J.; Yamagishi, F. G.; Garito, A. F.; Heeger, A. J. *Solid State Commun.* **1973**, *12*, 1125.
(16) Jérome, D.; Mazaud, A.; Ribault, M.; Bechgaard, K. *J. Phys. Lett.* **1980**, *41*, L95.
(17) Bechgaard, K.; Jacobsen, S.; Mortensen, K.; Pedersen, H. J.; Thorup, N. *Solid State Commun.* **1980**, *33*, 1119.
(18) Mizuno, M.; Cava, M. P. *J. Org. Chem.* **1978**, *43*, 416.
(19) Kikuchi, K.; Kikuchi, M.; Namiki, T.; Saito, K.; Ikemoto, I.; Murata, K.; Ishiguro, T.; Kobayashi, K. *Chem. Lett.* **1987**, 931.
(20) Papavassillou, G. C.; Mousdis, G. A.; Zamboni, J. S.; Terzis, A.; Hountas, A.; Hilti, B.; Mayer, C. W.; Pfeiffer, J. *Synth. Met.* **1988**, *27*, B379.
(21) Bossard, L.; Ribault, M.; Brousseau, M.; Valade, L.; Cassoux, P. *C. R. Acad. Sci. Paris* **1986**, *Ser. 2, 302*, 205.
(22) Williams, J. M.; Kini, A. M.; Wang, H. H.; Carlson, K. D.; Geiser, U.; Montgomery, L. K.; Pyrka, G. J.; Watkins, D. M.; Kommers, J. M.; Boryschuk, S. J.; Crouch, A. V. S.; Kwok, W. K.; Schirber, J. E.; Overmyer, D. L.; Jung, D.; Whangbo, M. H. *Inorg. Chem.* **1990**, *29*, 3272.
(23) Miller, J. S.; Calabresse, J. C.; Epstein, A. J.; Bigelow, W.; Zhang, J. H.; Reiff, W. M. *J. Chem. Soc., Chem. Commun.* **1986**, 1026.
(24) Pei, Y.; Verdaguer, M.; Kahn, O.; Sletten, J.; Renard, J. P. *J. Am. Chem. Soc.* **1986**, *108*, 7428.
(25) Miller, J. S.; Calabrese, J. C.; Rommelmann, H.; Chittapeddi, S. R.; Zhang, J. H.; Reiff, W. M.; Epstein, A. J. *J. Am. Chem. Soc.* **1987**, *109*, 769.
(26) Miller, J. S.; Epstein, A. J.; Reiff, W. M. *Chem. Rev. (Washington, D.C.)* **1988**, *88*, 201.
(27) Manriquez, J. M.; Yee, G. T.; McLean, R. S.; Epstein, A. J.; Miller, J. S. *Science* **1991**, *252*, 1415.
(28) Ferlay, S.; Mallah, T.; Ouahes, R.; Veillet, P.; Verdaguer, M. *Nature* **1995**, *378*, 701.
(29) Mallah, T.; Thiébaut, S.; Verdaguer, M.; Veillet, P. *Science* **1993**, *262*, 1554.
(30) Williams, J. M. *Prog. Inorg. Chem.* **1985**, *33*, 183.
(31) Lacroix, P.; Kahn, O.; Gleizes, A.; Valade, L.; Cassoux, P. *New J. Chem.* **1984**, *8*, 643.
(32) Gama, V.; Almeida, M.; Henriques, R. T.; Santos, I. C.; Domingos, A. *J. Phys. Chem.* **1991**, *95*, 4263.
(33) Gama, V.; Heniques, R. T.; Bonfait, G.; Almeida, M.; Meetsma, A.; Smaalen, S. V.; Boer, J. L. *J. Am. Chem. Soc.* **1992**, *114*, 1987.
(34) Miller, J. S.; Epstein, A. J.; Reiff, W. M. *Science* **1988**, *240*, 40.
(35) Broderick, W. E.; Thomson, J. A.; Day, E. P.; Hoffman, B. M. *Science* **1990**, *249*, 401.
(36) Eichorn, D. M.; Skee, D. C.; Broderick, W. E.; Hoffman, B. M. *Inorg. Chem.* **1993**, *32*, 491.
(37) Davison, A.; Holm, H. R. *Inorg. Synth.* **1967**, *10*, 8.
(38) Ouahab, L.; Bencharif, M.; Grandjean, D. *C. R. Acad. Sci. Paris* **1988**, *307*, *Ser. II*, 749.
(39) Mhanni, A.; Ouahab, L.; Peña, O.; Grandjean, D.; Garrigou-Lagrange, C.; Delhaes, P. *Synth. Met.* **1991**, *41*−*43*, 1703.
(40) Triki, S.; Ouahab, L.; Padiou, J.; Grandjean, D. *J. Chem. Soc., Chem. Commun.* **1989**, 1068.
(41) Triki, S.; Ouahab, L.; Halet, J. F.; Peña, O.; Padiou, J.; Grandjean, D.; Garrigou-Lagrange, C.; Delhaes, P. *J. Chem. Soc., Dalton Trans.* **1992**, 1217.
(42) Ouahab, L.; Bencharif, M.; Mhanni, A.; Pelloquin, D.; Halet, J. F.; Peña, O.; Padiou, J.; Grandjean, D.; Garrigou-Lagrange, C.; Amiell, J.; Delhaès, P. *Chem. Mater.* **1992**, *4*, 666.
(43) Bellito, C.; Attanazio, D.; Bonamico, M.; Fares, V.; Imperatori, P.; Patrizio, S. *Mater. Res. Soc. Proc.* **1990**, *173*, 143.
(44) Attanasio, D.; Bellitto, C.; Bonamico, M.; Fares, V.; Imperatori, P. *Gazz. Chim. Ital.* **1991**, *121*, 155.
(45) Bellitto, C.; Bonamico, M.; Staulo, G. *Mol. Cryst. Liq. Cryst.* **1993**, *232*, 155.
(46) Davidson, A.; Boubekeur, K.; Pénicaud, A.; Auban, P.; Lenoir, C.; Batail, P.; Hervé, G. *J. Chem. Soc., Chem. Commun.* **1989**, 1373.
(47) Ouahab, L.; Triki, S.; Grandjean, D.; Bencharif, M.; Garrigou-Lagrange, C.; Delhaès, P. In *Lower-Dimensional Systems and Molecular Electronics*; Metzger, R. M., Day, P., Papavassillou, G. C., Eds.; NATO-ASI Series; Plenum Press: New York, 1991; Vol. B248, p 185.
(48) Gómez-García, C. J.; Borras-Almenar, J. J.; Coronado, E.; Delhaes, P.; Garrigou-Lagrange, C.; Baker, L. C. W. *Synth. Met.* **1993**, *55*−*57*, 2027.
(49) Gómez-García, C. J.; Coronado, E. *Comm. Inorg. Chem.* **1995**, *17/5*, 255.
(50) Gómez-García, C. J.; Coronado, E.; Triki, S.; Ouahab, L.; Delhaès, P. *Synth. Met.* **1993**, *55*−*57*, 1787.
(51) Gómez-García, C. J.; Coronado, E.; Triki, S.; Ouahab, L.; Delhaès, P. *Adv. Mater.* **1993**, *4*, 283.
(52) Ouahab, L. In *Polyoxometalates: from Platonic Solids to Anti-retroviral activity*; Pope, M. T., Müller, A., Eds.; Kluwer Academic Publishers: Dordrecht, The Netherlands, 1994.
(53) Triki, S.; Ouahab, L.; Grandjean, D.; Amiell, J.; Garrigou-Lagrange, C.; Delahes, P.; Fabre, J. M. *Synth. Met.* **1991**, *41*−*43*, 2589.
(54) Gómez-García, C. J.; Ouahab, L.; Gimenez-Saiz, C.; Triki, S.; Coronado, E.; Delhaès, P. *Angew. Chem., Int. Ed. Engl.* **1994**, *33*−*2*, 223.
(55) Gómez-García, C. J.; Gimenez-Saiz, C.; Triki, S.; Coronado, E.; Le Magueres, P.; Ouahab, L.; Ducasse, L.; Sourisseau, C.; Delhaès, P. *Inorg. Chem.* **1995**, *34*, 4139.
(56) Le Maguerès, P.; Ouahab, L.; Golhen, S.; Peña, O.; Gomez-Garcia, C. J.; Delhaès, P. *Inorg. Chem.* **1994**, *33*, 5180.
(57) Rimbaud, C.; Ouahab, L.; Sutter, J. P.; Kahn, O. *Mol. Cryst. Liq. Cryst.*, in press.
(58) Souchay, P. *Ions Minéraux Condensés*; Masson: Paris, 1969.
(59) Pope, M. T. *Heteropoly and Isopoly Oxometalates*; Springer-Verlag: New York, 1983.
(60) Evans, H. T., Jr. *Perspectives Struct. Chem.* **1971**, *4*, 1.
(61) Pope, M. T., Müller, A., Eds. *Polyoxometalates: from Platonic Solids to Anti-retroviral activity*; Kluwer Academic Publishers: Dordrecht, The Netherlands, 1994.
(62) Pope, M. T.; Müller, A. *Angew. Chem., Int. Ed. Engl.* **1991**, *30*, 34.
(63) Iwamura, H.; Koga, N. *Acc. Chem. Res.* **1993**, *26*, 346.
(64) Fettouhi, M.; Ouahab, L.; Hagiwara, M.; Codjovi, E.; Kahn, O.; Constant-Machado, H.; Varret, F. *Inorg. Chem.* **1995**, *34*, 4152.
(65) Fujita, I.; Teki, Y.; Takui, T.; Kinishita, T.; Itoh, K.; Miko, F.; Sawaki, Y. *J. Am. Chem. Soc.* **1990**, *112*, 4047.
(66) Nakamura, N.; Inoue, K.; Iwamura, H.; Fulioka, T.; Sawaki, Y. *J. Am. Chem. Soc.* **1992**, *114*, 1484.
(67) Iwamura, H. *Mol. Cryst. Liq. Cryst.* **1993**, *232*, 233.
(68) Chiarelli, R.; Novak, M. A.; Rassat, A.; Tholence, J. L. *Nature* **1993**, *363*, 147.
(69) Turek, P.; Nozawa, K.; Shiomi, D.; Awaga, K.; Inabe, T.; Maruyama, Y.; Kinoshita, M. *Chem. Phys. Lett.* **1991**, *180*, 327.
(70) Tamura, M.; Yakazawa, Y.; Shiomi, D.; Nozawa, K.; Hosokoshi, Y.; Ishikawa, M.; Takahashi, M.; Kinoshita, M. *Chem. Phys. Lett.* **1991**, *186*, 401.
(71) Pei, Y.; Kahn, O.; Aebersold, M. A.; Ouahab, L.; Le Berre, F.; Pardi, L.; Tholence, J. L. *Adv. Mater.* **1994**, *6*, 681.
(72) Lang, A.; Pei, Y.; Ouahab, L.; Kahn, O. *Adv. Mater.* **1996**, *8*, 60.
(73) Keggin, J. F. *Proc. R. Soc. London, Ser. A* **1934**, *144*, 75.
(74) Lindqvist, I.; Aronsson, T. *Ark. Kemi* **1953**, *5*, 247.
(75) Lindqvist, I.; Aronsson, T. *Ark. Kemi* **1954**, *57*, 49.
(76) Anderson, J. S. *Nature (London)* **1937**, *140*, 850.

(77) Evans, H. T., Jr. *J. Am. Chem. Soc.* **1948**, *70*, 1291.
(78) Dawson, B. *Acta Crystallogr.* **1953**, *6*, 113.
(79) Finke, R. G.; Droege, M. W.; Domaille, P. J. *Inorg. Chem.* **1987**, *26*, 3886.
(80) Evans, H. T., Jr.; Tourné, C. M.; Tourné, G. F.; Weakley, T. J. R. *J. Chem. Soc., Dalton Trans.* **1986**, 2699.
(81) Weakley, T. J. R.; Finke, R. G. *Inorg. Chem.* **1990**, *29*, 1235.
(82) Gomez Garcia, C. J.; Borras-Almenar, J. J.; Coronado, E.; Ouahab, L. *Inorg. Chem.* **1994**, *33*, 4016.
(83) Launay, J. P. *J. Inorg. Nucl. Chem.* **1976**, *18*, 807.
(84) Baker, L. C. W.; Figgis, J. S. *J. Am. Chem. Soc.* **1970**, *92*, 3794.
(85) Shaikh, S. N.; Zubieta, J. *Inorg. Chem.* **1986**, *25*, 4613.
(86) Proust, A.; Fournier, M.; Thouvenot, R.; Gouzerh, P. *Inorg. Chim. Acta* **1994**, *215*, 61.
(87) Chorghade, G. S.; Pope, M. T. *J. Am. Chem. Soc.* **1987**, *109*, 5134.
(88) Strong, J. B.; Ostrander, R.; Rheingold, A. L.; Maatta, E. *J. Am. Chem. Soc.* **1994**, *116*, 3601.
(89) Figgis, B. N.; Forsyth, J. B.; Reynolds, P. A. *Inorg. Chem.* **1987**, *26*, 101.
(90) Figgis, B. N.; Kusharski, E. S.; Vrtis, M. *J. Am. Chem. Soc.* **1993**, *115*, 176.
(91) Michaut, C.; Ouahab, L.; Bergerat, P.; Kahn, O.; Bousseksou, A. *J. Am. Chem. Soc.* **1996**, *118*, 3610.
(92) Jaselskis, B.; Dielh, H. *J. Am. Chem. Soc.* **1958**, *80*, 4197.
(93) Mascharak, P. K. *Inorg. Chem.* **1986**, *25*, 245.
(94) Le Maguerès, P.; Ouahab, L.; Briard, P.; Even, J.; Bertault, M.; Toupet, T.; Rámos, J.; Gómez-García, C. J.; Delhaès, P. *Mol. Cryst. Liq. Cryst.*, in press.
(95) Graja, A. *Low, Dimensional Organic Conductors*; World Scientific: Utopia, Singapore, 1992.
(96) Cowan, D. O.; Fortkort, J. A.; Metzger, R. M. In *Lower Dimensionnal Systems and Molecular Electronics*; Metzger, R. M., Day, P., Papavassillou, G. C., Eds.; NATO-ASI Series; Plenum Press: New York, 1991; Vol. B248, p 1, and references therein.
(97) Delhaes, P. In *Lower Dimensionnal Systems and Molecular Electronics*; Metzger, R. M., Day, P., Papavassillou, G. C., Eds.; NATO-ASI Series; Plenum Press: New York, 1991; Vol. B248, p 43, and references therein.
(98) Ouahab, L.; Batail, P.; Perrin, C.; Garrigou-Lagrange, C. *Mater. Res. Bull.* **1986**, *51*, 1223.
(99) Batail, P.; Ouahab, L.; Pénicaud, A.; Lenoir, C.; Perrin, A. *C. R. Acad. Sci. Paris* **1987**, *Ser. II*, *304*, 1111.
(100) *Research Frontiers in Magnetochemistry*; O'Connor, C. J., Ed.; 1994.
(101) Caneschi, A.; Gatteschi, D.; Rey, P.; Sessoli, R. *Inorg. Chem.* **1988**, *27*, 1756.
(102) Caneschi, A.; Gatteschi, D.; Renard, J. P.; Rey, P.; Sessoli, R. *Inorg. Chem.* **1989**, *28*, 3314.
(103) Caneschi, A.; Gatteschi, D.; Renard, J. P.; Rey, P.; Sessoli, R. *J. Am. Chem. Soc.* **1989**, *111*, 785.
(104) Stumpf, H.; Ouahab, L.; Pei, Y.; Grandjean, D.; Kahn, O. *Science* **1993**, *261*, 447.
(105) Stumpf, H.; Ouahab, L.; Pei, Y.; Bergerat, P.; Kahn, O. *J. Am. Chem. Soc.* **1994**, *116*, 3866.
(106) Lepage, I. J.; Breslow, R. *J. Am. Chem. Soc.* **1987**, *109*, 6412.
(107) McConnell, H. M. *Proc. Robert A. Welch Found. Conf. Chem. Res.* **1967**, *11*, 164.
(108) Torrance, J. B.; Oostra, S.; Nazzal, A. *Synth. Met.* **1987**, *29*, 709.
(109) Dormann, E.; Nowak, M. J.; Williams, K. A.; Angus, R. O.; Wudl, F. *J. Am. Chem. Soc.* **1987**, 2594.
(110) Broderick, W. E.; Hoffman, B. M. *J. Am. Chem. Soc.* **1991**, *113*, 6334.
(111) Alvarez, S.; Vicente, R.; Hoffman, R. *J. Am. Chem. Soc.* **1985**, *107*, 6253.
(112) Fettouhi, M.; Ouahab, L.; Codjovi, E.; Kahn, O. *Mol. Cryst. Liq. Cryst.* **1995**, *273*, 29.
(113) Broderick, W. E.; Thompsoon, J. A.; Godfrey, M. R.; Sabat, M.; Hoffman, M. *J. Am. Chem. Soc.* **1989**, *111*, 7656.
(114) Golhen, S.; Ouahab, L.; Grandjean, D.; Molinié, P., manuscript in preparation.
(115) Kahn, O. *Struct. Bonding* **1987**, *68*, 89.
(116) Kahn, O. *Angew. Chem., Int. Ed. Engl.* **1985**, *24*, 834.
(117) Kahn, O.; Galy, J.; Journeaux, Y.; Jaud, J.; Morgenstern-Badarau, I. *J. Am. Chem. Soc.* **1982**, *104*, 2165.
(118) Zhedlev, A.; Barone, V.; Bonnet, M.; Delley, B.; Grand, A.; Ressouch, E.; Rey, P.; Subra, R.; Schweitzer, J. *J. Am. Chem. Soc.* **1994**, *116*, 2019.
(119) Veciana, J.; Cirujeda, J.; Rovira, C.; Vidal-Gancedo, J. *Adv. Mater.* **1995**, *7*, 221.
(120) Awaga, K.; Inabe, T.; Nagashima, U.; Nakamura, T.; Matsumoto, M.; Kawabata, Y.; Maruyama, Y. *Chem. Lett.* **1991**, 1777.
(121) Awaga, K.; Inabe, T.; Maruyama, Y.; Nakamura, T.; Matsumoto, M. *Chem. Phys. Lett.* **1992**, *195*, 21.
(122) Awaga, K.; Yamagushi, A.; Okuno, T.; Inabe, T.; Nakamura, T.; Matsumoto, T.; Maruyama, Y. *J. Mater. Chem.* **1994**, *4*, 1377.
(123) Awaga, K.; Okuno, T.; Yamagushi, Y.; Hasegawa, M.; Inabe, T.; Maruyama, Y. *Phys. Rev. B* **1994**, *49*, 3975.
(124) Kollmar, C.; Kahn, O. *Acc. Chem. Res.* **1993**, *26*, 259.
(125) Kahn, O. *Comm. Condens. Matter. Phys.* **1994**, *17*, 39.
(126) Elliott, J. R. In *Magnetism*; Rado, Suhl, Eds.; Academic Press: New York, 1965; Vol. IIA, p 385.
(127) Heeger, A. J. *Solid State Phys. B* **1969**, *23*, 283.
(128) Henriques, R. T.; Alcacer, L.; Pouget, J. P.; Jérôme, D. *J. Phys. C, Solid State Phys.* **1984**, *17*, 5197.
(129) Bray, J. W.; Interrante, L. V.; Jacobs, I. S.; Bonner, J. C. The spin Peierls Transition. In *Extended Linear Chain Compounds*; Miller, J. S., Ed.; Plenum Press: New York, 1982, and references therein.
(130) Batail, P.; Ouahab, L.; Torrance, J. B.; Pylmann, M. L.; Parkin, S. S. P. *Solid State Commun.* **1985**, *55−7*, 597.
(131) Aumuller, A.; Erk, P.; Klebe, G.; Hunig, S.; Shutz, J. U.; Werener, H. P. *Angew. Chem., Int. Ed. Engl.* **1986**, *25*, 740.
(132) Kobayashi, A.; Kato, R.; Kobayashi, H.; Mori, T.; Inokuchi, H. *Solid State Commun.* **1987**, *64*, 45.
(133) Ogawa, M. Y.; Martinsen, J.; Palmer, S. M.; Stanton, J. L.; Tanaka, J.; Greene, R. L.; Hoffman, B. M.; Ibers, J. A. *J. Am. Chem. Soc.* **1987**, *109*, 1115.
(134) Lequan, M.; Lequan, R. M.; Hauw, C.; Gaultier, J.; Maceno, G.; Delhaès, P. *Synth. Met.* **1987**, *19*, 409.
(135) Mori, T.; Wang, P.; Imaeda, K.; Enoki, T.; Inokuchi, H.; Sakai, F.; Saito, G. *Synth. Met.* **1988**, *27*, A451.
(136) Mallah, T.; Hollis, C.; Kurmoo, M.; Day, P.; Allan, M.; Friend, R. H. *J. Chem. Soc., Dalton Trans.* **1990**, 859.
(137) Day, P.; Kurmoo, M.; Mallah, T.; Marsden, I. R.; Friend, R. H.; Pratt, F. L.; Hayes, W.; Chasseau, D.; Gaultier, J.; Bravic, G.; Ducasse, L. *J. Am. Chem. Soc.* **1992**, *114*, 10722.
(138) Kobayashi, A.; Udagawa, T.; Tomita, H.; Naito, T.; Kobayashi, H. *Chem. Lett.* **1993**, 2179.
(139) Graham, A. W.; Kurmoo, M.; Day, P. *J. Chem. Soc., Chem. Commun.* **1995**, 2061.
(140) Kobayashi, H.; Tomita, H.; Naito, T.; Kobayashi, A.; Sakai, F.; Watanabe, T.; Cassoux, P. *J. Am. Chem. Soc.* **1996**, *118*, 368.
(141) Le Maguerès, P.; Ouahab, L.; Conan, N.; Gomez-Garcia, C. J.; Delhaes, P.; Even, J.; Bertault, M. *Solid State Commun.* **1996**, *97/1*, 27.
(142) Prados, R. A.; Pope, M. T. *Inorg. Chem.* **1976**, *15*, 2547.
(143) Launay, J. P.; Fournier, M.; Sanchez, C.; Livage, J.; Pope, M. T. *Inorg. Nucl. Chem. Lett.* **1980**, *16*, 257.
(144) Barrows, J. N.; Pope, M. T. In *Electron Transfer in Biology and the Solid State*; Johnson, M. K., King, R. B., Kurtz, D. M., Kutal, C., Norton, M. L., Scott, R. A., Eds.; Advances in Chemistry Series 226; American Chemical Society: Washington, D.C., 1990.
(145) Che, M.; Fournier, M.; Launay, J. P. *J. Chem. Phys.* **1979**, *71-(4)*, 1954.
(146) Sanchez, C.; Livage, J.; Launay, J. P.; Fournier, M. *J. Am. Chem. Soc.* **1983**, *105*, 6817.
(147) Bouherour, S.; Ouahab, L.; Peña, O.; Padiou, J.; Grandjean, D. *Acta Crystallogr.* **1989**, *C45*, 371.
(148) Doublet, M. L.; Canadell, E.; Shibaeva, R. P. *J. Phys. I France* **1994**, *4*, 1479.
(149) Moldenhauer, J.; Horn, C.; Pokhodonia, H. I.; Schweitzer, D.; Heinen, I. Keller, H. J. *Synth. Met.* **1993**, *60*, 31.
(150) Moldenhauer, J.; Horn, Ch.; Pokhodonia, H. I.; Schweitzer, D.; Heinen, I.; Keller, H. J. *Synth. Met.* **1993**, *60*, 31.
(151) For a general review see: Gütlich, P.; Hauser, A.; Spiering, H. *Angew. Chem., Int. Ed. Engl.* **1994**, *33*, 2024 and references therein.
(152) Cambi, L.; Cagnasso, A. *Atti Accad. Naz. Lincei* **1931**, *13*, 809.
(153) Claude, R.; Real, J. A.; Zarembowitch, J.; Kahn, O.; Grandjean, D.; Boukhadden, K.; Varret, F.; Dworkin, A. *Inorg. Chem.* **1990**, *29*, 4442.
(154) Roux, C.; Zarembowitch, J.; Gallois, B.; Granier, T.; Claude, R. *Inorg. Chem.* **1994**, *33*, 2273.
(155) Sutter, J. P.; Fettouhi, M.; Michaut, C.; Li, L.; Ouahab, L.; Kahn, O. *Angew. Chem., Int. Ed. Engl.* **1996**, *35*, 2113.

CM9701217